Journal of Statistical Physics, Vol. 61, Nos. 1/2, 1990

High-Temperature Series for Scalar-Field Lattice Models: Generation and Analysis

Bernie G. Nickel[1] **and J. J. Rehr**[2]

Received May 18, 1986; final May 16, 1990

An implementation of the free-embedding scheme for high-temperature series generation on the body-centered cubic family of lattices in arbitrary dimension d is described. Series to order 21 in inverse temperature are tabulated for several scalar field models, both for the magnetic susceptibility and for the second moment of the spin correlation function. The critical behavior of a family of 3-dimensional "double Gaussian" models, which interpolate continuously between the spin-1/2 Ising model and the Gaussian model, is analyzed in detail away from the Gaussian model limit using confluent inhomogeneous second-order differential approximants. With our best estimate of the correction-to-scaling exponent, $\theta = 0.52 \pm 0.03$, the leading exponents for the susceptibility and correlation length for this family are consistent with universality and are given by $\gamma = 1.237 \pm 0.002$ and $\nu = 0.630 \pm 0.0015$, respectively, and $\eta = 2 - \gamma/\nu = 0.0359 \pm 0.0007$.

KEY WORDS: Ising model; series generation; series analysis; critical exponents; universality.

1. INTRODUCTION AND SUMMARY OF RESULTS

Estimates of critical exponents deduced from high-temperature series on 3-dimensional lattices have been puzzling for a number of years. Contrary to the expectations of renormalization-group theory, there has been evidence both for the failure of hyperscaling[1] and the absence of universality. The latter is suggested by a discrepancy between the "classical" estimates of the susceptibility exponent $\gamma = 1.250 \pm 0.003$[2] and the correlation length exponent $\nu = 0.638^{+0.002}_{-0.001}$,[3] and the most recent space

[1] Department of Physics, University of Guelph, Guelph N1G 2W1, Ontario, Canada.
[2] Department of Physics, FM-15, University of Washington, Seattle, Washington 98195.

0022-4715/90/1000-0001$06.00/0

continuum ϕ^4-model estimates.[4] These are $\gamma = 1.241 \pm 0.002$ and $\nu = 0.6300 \pm 0.0015$, based on Borel resummation of coupling constant perturbation expansions, and $\gamma = 1.2390 \pm 0.0025$ and $\nu = 0.6310 \pm 0.0015$, based on Borel resummation of ε-expansion series supplemented by exact results in two dimensions. However, the numerical arguments for or against hyperscaling and universality appear to depend on the method used to analyze series expansions of limited length. Each method inevitably builds in particular "function biases" and, as a consequence, yields analysis-dependent results.[3] It is therefore hoped that with longer series, less function-biased analyses might be undertaken which will either confirm, say, the absence of universality or resolve the apparent discrepancies and show how they arose from certain biases.

Although the prospects for extending these series for general 3-dimensional lattices are not encouraging, a great simplification in the high-temperature series generation process is possible for the body-centered cubic (bcc) lattice.[5] Exploiting this simplification, Nickel reported new 21-term spin-1/2 Ising series for the susceptibility and correlation length at Cargèse in 1980.[9] Also reported was a preliminary analysis of these and corresponding higher-spin-S series which showed that the "classical" exponent estimates were seriously in error and that the new estimates appeared to be consistent with universality. Since then, series for other models have been derived and many more analyses[10–21] of these bcc series have been reported; ref. 21 contains a recent discussion. Here we finally (!) report the details of this series derivation, tabulate series coefficients for models we hope will be of general interest, and present an analysis which in preliminary stages was reported at Stat Phys XIV,[22] Rutgers,[23] and APS[24] meetings.

Our analysis is based on confluent inhomogeneous second-order differential approximants which, by allowing for a correction-to-scaling term in a simple form and an analytic background, can (potentially) yield an unbiased test of universality. However, in practice we can only obtain the high precision of about three decimal places for γ and ν and not quite two decimal places for the correction-to-scaling exponent θ by comparing different models and "forcing" universality by a best-fit procedure. As opposed to other methods of series analysis which usually focus on a single thermodynamic quantity, our approach uses both susceptibility and correlation-length series and makes use of several internal consistency checks to help reduce the effects of function bias. Our best estimates of the critical exponents are consistent with (1) a common correction-to-scaling

[3] See, for example, the discussion of hyperscaling in ref. 5, or compare the analyses by Gaunt and Sykes[6] and Zinn-Justin.[7] A review of early work has been compiled by Gaunt.[8]

exponent θ for a family of models; (2) the same critical temperature for both the susceptibility and correlation length series for a given model; (3) a common value of y^*, i.e., the model parameter at which the leading correction-to-scaling vanishes; and (4) universality of the subdominant amplitude ratio. The use of confluent approximants is essential to our method; Guttmann[20] also carried out a differential approximant analysis without explicitly including a confluent singularity in each approximant and obtained rather different results. Inhomogeneous approximants have been found to be particularly important in reducing the overall scatter of the critical exponent estimates, especially for the ξ^2 series. Such inhomogeneous approximants automatically incorporate an analytic background and remove spurious effects of the leading terms in a series. The effect of the inhomogeneous term on critical exponent estimates is a reduction of about 0.002 in both γ and 2ν. Our results are, within error limits, consistent with other analyses that are also unbiased in their exponent choices and that explicitly depend on model comparisons.[13] A common conclusion is that for the spin-1/2 Ising model, the correction-to-scaling term, though small, *cannot* be neglected. On the other hand, our conclusion is similar to that reached by Zinn-Justin[10] and is worth stressing; namely, that even with the long series now available, any analysis based solely on the spin-1/2 series *cannot predict* the presence of a correction-to-scaling term.[4]

A summary of this paper in somewhat more detail is as follows. As mentioned in ref. 5, the evaluation of graph embedding constants, which for most lattices is the most time-consuming part of the series calculation, becomes almost trivial on the family[5] of d-dimensional lattices for which the interactions couple fields bilinearly on lattice sites separated by any of the 2^d vector displacements $(\pm 1, \pm 1, \ldots, \pm 1)$. Another consequence of this factorization is that the high-temperature susceptibility series can be written as

$$\chi(K) = \sum_{n=0} \frac{1}{n!} K^n \sum_{\sum i m_i = n+1} \left(\prod_{i=1} (\mu_{2i})^{m_i} \right) \times \sum_g [E_g(\{m_i\})]^d W_g(\{m_i\}) \tag{1.1}$$

[4] Both Mellin transform[11] and 5-point fits[16] fail to find significant corrections for the spin-1/2 case. The trend of the D log Padé estimates[9] is suggestive of a correction, but of course each approximant specifically excludes such a term. Finally, for spin 1/2, second-order differential approximants[22] fit just as easily with $\theta \equiv \gamma$, i.e., an analytic background, as with $\theta \approx 0.5$.

[5] This "bcc family" includes a pair of sites ($d=0$), the linear chain ($d=1$), the simple quadratic lattice ($d=2$), the bcc ($d=3$), and higher-dimensional generalizations. The basis for the simplification is a factorizability described in Section 2, which reduces the d-dimensional embedding calculation to that in one dimension.

and the second moment of the 2-point correlations as

$$M_2(K) = \sum_{n=0} \frac{1}{n!} K^n \sum_{\sum i m_i = n+1} \left[\prod_{i=1} (\mu_{2i})^{m_i} \right] \times \sum_g [E_g(\{m_i\})]^{d-1} F_g(\{m_i\}) W_g(\{m_i\}) \tag{1.2}$$

where K is the inverse temperature and $\{\mu_{2i}\}$, the cumulant moments of the single-site field distribution [see Eqs. (2.1) and (2.6)], are the physical model-dependent parameters; the dimension d appears only as an exponent, while the remaining quantities are integer constants that can be given a graphical interpretation. In particular, the m_i are the number of vertices of order $2i$ in 2-rooted graphs of type g; $E_g(\{m_i\})$ is a one-dimensional embedding constant or zeroth moment in root separation, while $F_g(\{m_i\})$ is the second moment in root separation. $W_g(\{m_i\})$ is a sum of symmetry-related weight factors of all graphs with the same embedding constant moments E_g and F_g. A few technical details of the computer program that determines these integer constants through order $n = 21$ are also described in Section 2.

The data for χ and M_2 for the order K^{21} calculation comprise nearly 100,000 entries of the constants E_g, F_g, and W_g and can be conveniently transferred only via magnetic tape. To make these results more directly accessible, we specialize the general scalar models, characterized by the set of cumulant moments $\{\mu_{2i}\}$, to models in which the single-site field distribution is parametrized by a single variable y. The series for χ and M_2 can then be written as

$$\chi(K, y) = \sum K^n A_n(y), \qquad M_2(K, y) = \sum K^n B_n(y) \tag{1.3}$$

Furthermore, a number of physically interesting models exist for which the $A_n(y)$ and $B_n(y)$ are expressible as polynomials of order approximately n. Such models, which include spin-S Ising, Blume–Capel,[25] Klauder,[26] and double-Gaussian[23] or range,[27] are described in Section 3 and a few representative tables of coefficients of double power series in K and y are listed in the Appendix. Readers interested in other models should contact the authors.

With the much longer series now available one can reexamine the previous Ising model critical exponent estimates using a number of methods ranging from such commonly used approaches as the ratio and D log Padé to the more recently developed second-order differential approximants[28] and (two-variable) partial differential approximants.[18, 29] Each method has its relative merits. For example, the conventional D log Padé is easy to

apply and directly separates the effects of unphysical singularities from the critical singularities of physical interest. Unfortunately, the method assumes the absence of correction-to-scaling terms discussed by Wegner,[30] and this can lead to systematic errors in the leading critical exponent estimates. Exponents from D log Padé approximants[9] to 21-term spin-S Ising series are spin dependent and taken at face value suggest the absence of universality. On the other hand, the two-variable partial differential approximant method[13] as applied to the double-Gaussian and Klauder series assumes the presence of a single correction-to-scaling term in the scaling form predicted by renormalization-group theory.[30] Since this method uses all the information in each two-variable series simultaneously, it will probably yield the best possible exponent estimates if the renormalization-group hypothesis is correct and if higher-order corrections are sufficiently small. Of course, it is conceivable that the observed scatter in those estimates[13] is a response to model-dependent exponents, and thus in a sense the method is not a test of universality. The partial differential approximant method of ref. 18 is based on the same scaling assumption, but uses more limited information, namely two single-variable series $\chi(K)$ and $\partial\chi(K)/\partial y$ for a given model parameter y. Exponent estimates have also been made[19] using inhomogeneous first-order differential approximants and determining, self-consistently, a value y^* at which the leading nonanalytic corrections-to-scaling in χ vanish. Although not a test of universality, the resulting exponents have been used to check the validity of hyperscaling.

In the present paper we concentrate on analysis of the double-Gaussian series by single-variable confluent inhomogeneous second-order differential approximants. This simple generalization of the D log Padé method assumes that a single correction-to-scaling term is important. Also, as described in Section 4, χ, M_2, and the correlation length squared $\xi^2 \propto M_2/\chi$ are assumed to have critical behavior

$$F(K) \sim \begin{cases} A_F\left(1-\dfrac{K}{K_c}\right)^{-\gamma_F}\left[1+a_F\left(1-\dfrac{K}{K_c}\right)^{\theta_F}\right]+B_F, & K \approx K_c \\ C_F\left(1+\dfrac{K}{K_c}\right)^{1-a_F}+D_F, & K \approx -K_c \end{cases} \tag{1.4}$$

in the neighborhood of the ferromagnetic and antiferromagnetic critical points $K = \pm K_c$.[6]

[6] The second-order inhomogeneous differential approximants exhibit critical behavior of the form (1.4), in which the coefficients A_F, a_F, and B_F (C_F and D_F) are regular functions of K at K_c ($-K_c$). While it is not likely that the background term B_F contains the leading corrections beyond the $(1-K/K_c)^\theta$ term, its inclusion tends to give more stable estimates for γ_F and θ_F. This background term may also be the best polynomial approximation to additional important but slowly varying confluent corrections.

In principle one could determine without bias, other than the implicit function bias of a given method, estimates of K_c, γ_F, and θ_F for many different models and then reasonably decide whether universality is satisfied; i.e., whether the γ_F are model independent and the θ_F are both model and function independent. We find, not too surprisingly,[31] that such double exponential fitting is very unstable and that even longer series will be needed before one can hope to succeed in verifying universality with this naive approach. Thus, instead, we have adopted the procedure of fixing θ_F at a few discrete values and determining only K_c and γ_F. We find that there is a "best" value for $\theta_F = \theta \approx 0.52 \pm 0.03$, for which the exponents γ_F are most constant over a wide range of y parameter values in the double-Gaussian model. In this limited sense we do verify universality and find $\gamma_\chi \equiv \gamma = 1.237 \pm 0.002$, $\gamma_{\xi^2} \equiv 2\nu = 1.260 \pm 0.003$, and $\eta \equiv 2 - \gamma/\nu = 0.0359 \pm 0.0007$. It is not clear how much function bias remains in these results. While slightly lower than some estimates, our present exponents are consistent, within error bounds, with other analyses of the double-Gaussian model; e.g., $\gamma = 1.2385 \pm 0.0015$ from ref. 13, $\gamma = 1.237 \pm 0.003$ from ref. 14, $\gamma = 1.2378 \pm 0.0012$ from ref. 18 (we have doubled those authors' one-standard-deviation error estimates), and $\gamma = 1.2395 \pm 0.0004$ from ref. 19. Similarly, our results for ν are also consistent with other analyses; e.g., $\nu = 0.632 \pm 0.001$ from ref. 13, $\nu = 0.630 \pm 0.003$ from ref. 14, and $\nu = 0.6312 \pm 0.0006$ from ref. 18. Our value $1 - \alpha_\chi = 0.89 \pm 0.02$ is consistent with the hyperscaling relation $3\nu = 2 - \alpha$, but is too uncertain to be considered a significant test. By comparison, the inhomogeneous differential approximants of ref. 19 yield $1 - \alpha_\chi = 0.895 \pm 0.007$, for which the hyperscaling relation is satisfied to a precision of ± 0.01.

There is now little indication of an absence of universality or of a significant discrepancy between high-temperature series and field-theoretic results. Although earlier continuum ϕ^4-model estimates,[4] $\gamma = 1.241 \pm 0.002$ and $\eta = 0.031 \pm 0.004$, were only marginally in agreement with the lattice results, the latest estimates[4] derived from ε-expansions and exact results, $\gamma = 1.2390 \pm 0.0025$ and $\eta = 2 - \gamma/\nu = 0.0365 \pm 0.003$, are now consistent, within error limits. Additional support for universality is provided by studies of leading amplitude ratios.[19] Possible evidence for a lack of universality is that the correction-to-scaling amplitude ratio a_{ξ^2}/a_χ is weakly model dependent and near its maximum value $a_{\xi^2}/a_\chi \approx 1.7$ at the spin-1/2 Ising limit. This ratio is some 25% larger than the value of ≈ 1.3 estimated[32] for the continuum model; however, given the latest continuum model results, the value 1.3 is now suspect. Both the large magnitude and model dependence of a_{ξ^2}/a_χ are consistent with those found by Nickel and Dixon[14] based on Roskie's[12] quadratic mapping. The

estimate $a_{\xi^2}/a_\chi \approx 1.42 \pm 0.14$, obtained by Zinn-Justin[10] by a modified ratio method, is somewhat lower.

Overall, however, we believe that the analyses based on these new high-temperature series favor universality. The series are probably still too short to capture the true asymptotic behavior of the *correction-to-scaling* terms, especially since, as already mentioned, these cannot yet be predicted for the spin-1/2 Ising model treated in isolation. In view of this, we discuss in Section 5 considerations important for an extension of the present calculation to generate additional series terms.

2. SERIES GENERATION

The models considered in this paper are defined by the bcc family partition functions

$$Z = \prod_i \left[\int d\phi_i f(\phi_i^2) \exp(h_i \phi_i) \right] \exp\left(K \sum_{nn} \phi_i \phi_j \right) \tag{2.1}$$

where the sites $\mathbf{r}_i$ are either all even $(2l, 2m,...)$ or all odd $(2l+1, 2m+1,...)$ integer translations from the origin. The interaction couples "nearest" neighbor scalar fields ϕ_i, ϕ_j on sites separated by $(\pm 1, \pm 1,..., \pm 1)$. The 2-point correlation function in zero magnetic field h_i is

$$\langle \phi_i \phi_j \rangle = \frac{\partial^2}{\partial h_i \, \partial h_j} \ln Z \bigg|_{\{h_i = 0\}} \tag{2.2}$$

and its Fourier transform is the propagator or $\mathbf{q}$-dependent susceptibility

$$G(\mathbf{q}, K) = \chi_{\mathbf{q}} = \sum_j \langle \phi_i \phi_j \rangle \exp[i\mathbf{q} \cdot (\mathbf{r}_i - \mathbf{r}_j)] \tag{2.3}$$

Of particular interest is the uniform susceptibility $\chi = \chi_{\mathbf{q}=0}$ and the second moment of the spin correlations

$$M_2 = -\frac{\partial^2 \chi_{\mathbf{q}}}{\partial q_x^2} \bigg|_{\mathbf{q}=0} = \sum_j (x_i - x_j)^2 \langle \phi_i \phi_j \rangle \tag{2.4}$$

from which one can define the correlation length ξ via

$$\xi^2 = M_2 / 2\chi \tag{2.5}$$

Different models are distinguished by the single-site field distribution

function $f(\phi^2)$ or equivalently by its cumulant moments μ_{2n}, which are determined from the generating function,

$$\exp\left[\sum_n \frac{\mu_{2n}}{(2n)!} h^{2n}\right] = \int d\phi\, f(\phi^2) e^{h\phi} \tag{2.6}$$

A number of explicit choices for $f(\phi^2)$ are discussed in Section 3.

The coefficients of the expansion of $\chi_{\mathbf{q}}$ in powers of K can be represented as a graphical sum. Each graph consists of vertices (lattice sites) connected by bonds ["nearest" neighbor vectors $(\pm 1, \pm 1, \ldots, \pm 1)$], each of which is associated with a factor K. For the zero-magnetic-field expansion considered here, the number of bonds leaving each vertex, which is the order of the vertex, must be even. For this particular counting purpose an "external" bond is considered to be associated with each *root vertex* i and j in the average $\langle \phi_i \phi_j \rangle$ in (2.2). Also, for the free embedding scheme employed here, multiple bonds between pairs of vertices are allowed and distinct vertices in a graph are *not* restricted to correspond to distinct sites on the lattice. For a complete description of this scheme we refer the reader to the excellent article by Wortis.[33]

The numerical contribution of a particular graph is the product of a number of factors. Besides the factor K^n associated with the n internal bonds in the graph, a cumulant average μ_{2m} is associated with each vertex of order $2m$. Dividing these factors is the symmetry number of the graph, which is the number of distinct ways the internal bonds and vertices can be labeled and leave the graph topologically unchanged. Finally, one must multiply by the embedding constant, which is the total number of ways the vertices of the graph can be identified with lattice sites.

For example, the graphs shown in Figs. 1a and 1b contribute to $\chi_{\mathbf{q}}$ the values

$$\chi_{[1a]} = K^{18}\mu_2^6\mu_6^3\mu_8 \left(\frac{1}{3!\,5!}\right)\left(\frac{1}{2}\right) \sum_{\mathbf{r}_2,\ldots,\mathbf{r}_{10}} V_{13}V_{14}\cdots \exp[i\mathbf{q}\cdot(\mathbf{r}_1-\mathbf{r}_2)] \tag{2.7a}$$

$$\chi_{[1b]} = K^{18}\mu_2^3\mu_4^5\mu_6^2 \left(\frac{1}{3!}\right)^3\left(\frac{1}{2}\right) \sum_{\mathbf{r}_2,\ldots,\mathbf{r}_{10}} V_{13}V_{37}\cdots \exp[i\mathbf{q}\cdot(\mathbf{r}_1-\mathbf{r}_2)] \tag{2.7b}$$

where the V_{ij} are the "nearest" neighbor interactions, that is, $V_{ij}=1$ if $\mathbf{r}_i-\mathbf{r}_j=(\pm 1,\ldots,\pm 1)$ and zero otherwise. The 3! and 5! in Eq. (2.7) correspond to the possible permutations of the multiple bonds. The factor 1/2 in (2.7a) is the result of the vertex pair 7, 8 → 9, 10 relabeling symmetry, while in (2.7b) it is the 4 → 6 relabeling.

The presence of multiple bonds does not affect the lattice site sums, since $V_{ij}^2 = V_{ij}$. Furthermore, since all site locations are unrestricted, site

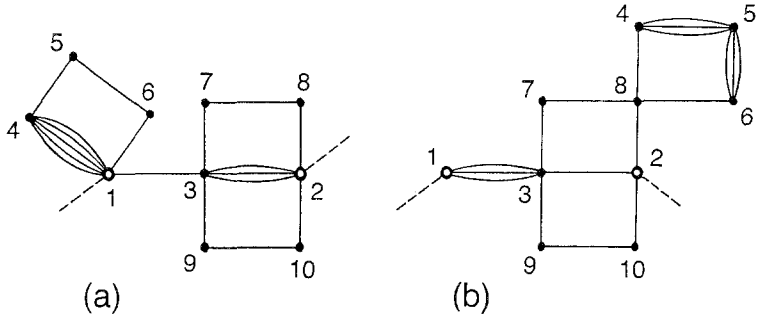

Fig. 1. Two order-K^{18} contributions to χ. The open circles labeled 1 and 2 are the roots, each solid line is a "nearest" neighbor bond associated with a factor K, and the dashed lines are the fictitious external bonds. All vertices are necessarily of even valence; all loops are of even length.

sums can also be evaluated simply in Fourier space. Using the inverse transform $V_{ij} = \int d^d q \, V_{\mathbf{q}} \exp[-i\mathbf{q} \cdot (\mathbf{r}_i - \mathbf{r}_j)](2\pi)^d$, where

$$V_{\mathbf{q}} = 2^d \cos q_x \cos q_y \cdots \tag{2.8}$$

is the Fourier transform of the "nearest" neighbor interaction V_{ij}, we obtain for the sums in both (2.7a) and (2.7b) the same three-loop integral

$$\sum_{\mathbf{r}_2,\ldots,\mathbf{r}_{10}} (\cdots) = V_{\mathbf{q}} \int \frac{d^d q_1}{(2\pi)^d} \int \frac{d^d q_2}{(2\pi)^d} V^3_{\mathbf{q}_1} V^3_{\mathbf{q}_2} V_{\mathbf{q}_1 - \mathbf{q}_2 + \mathbf{q}} \times \int \frac{d^d q_3}{(2\pi)^d} V^4_{\mathbf{q}_3} \tag{2.9}$$

The form for $V_{\mathbf{q}}$ in Eq. (2.8) is special to the bcc family; because of its factorizability, the expression (2.9) can be rewritten as a product $\prod_\alpha E_{q_\alpha}$ of d one-dimensional embedding constants, of the form

$$\begin{aligned} E_{q_\alpha} &= 2 \cos q_\alpha \int_0^{2\pi} \frac{dq_1}{2\pi} \int_0^{2\pi} \frac{dq_2}{2\pi} (2 \cos q_1)^3 (2 \cos q_2)^3 \\ &\quad \times 2 \cos(q_1 - q_2 + q_\alpha) \int_0^{2\pi} \frac{dq_3}{2\pi} (2 \cos q_3)^4 \\ &= 108 + 108 \cos 2q_\alpha \end{aligned} \tag{2.10}$$

where q_α is one of the components of $\mathbf{q}$. The evaluation of such one-dimensional embedding constants is usually most easily carried out in position space, but in any case is no longer the most time-consuming part of the graph calculation. This is the crucial feature that has made the present order-K^{21} calculation possible.

Quite generally, the contribution of a particular graph to χ_q is of the two possible forms

$$\chi_{[g]} = \frac{1}{n!} K^n \prod_m (\mu_{2m})^{c_m} \prod_\alpha \left(\sum_k e_k \begin{Bmatrix} \cos 2kq_\alpha \\ \cos(2k+1)q_\alpha \end{Bmatrix} \right) w \tag{2.11}$$

A complete description of this contribution is contained in the two linear and integer arrays c_m and e_k and the weight w, which, because of the factor $n!$, is also an integer. Graphs which are described by the same characteristic arrays c_m and e_k can be combined by adding together their respective weights w. This leads to a very considerable reduction of the number of tabular entries. Further reduction is possible if we specialize to the uniform susceptibility or the second moment; the array e_k can then be combined into the single number E_g as in (1.1) or the pair E_g and F_g as in (1.2). This reduction in storage requirements is the second most important feature that has made possible the present calculation.

In the remainder of this section we will describe a few technical details of the graph generation program. We have used the 2-point renormalization scheme as outlined by Wortis,[33] with one basic difference: that we never explicitly specify the field distribution function $f(\phi^2)$ and hence the moments $\{\mu_{2m}\}$. Instead, the equivalent information is always stored in arrays like c_m in (2.11) which specify the number of vertices of various orders.

The program divides roughly into five parts. First, a table of elementary 2-rooted, 2-irreducible graphs is generated. Second, the bonds in these graphs are replaced in all possible ways by 2-rooted, 1-irreducible segments to produce a table of elementary 2-rooted, 1-irreducible contributions. Third, another program segment generates 2-rooted nodal and ladder contributions which, when combined with the elementary contributions, yields a table of all 2-rooted, 1-irreducible contributions. Fourth, the two roots are collapsed to a single root to generate vertex insertions. These are self-consistently iterated to generate a complete table of 1-rooted contributions with bare vertices. Fifth, the 1-root contributions are used as replacements for the vertices in the 2-rooted, 1-irreducible table to generate all 2-rooted contributions with bare vertices. These last two tables constitute the information from which χ and M_2 can be obtained via (1.1) and (1.2).

The description of the entire program would be too long and not particularly instructive. Instead, we outline below the third segment to give a flavor of the data-handling techniques we have employed. Some additional remarks may be found in Section 5, where we discuss the prospects for a higher-order calculation.

Assume that a table of low-order elementary, nodal, and ladder con-

tributions exists. A particular entry contains the following information elements: (1) order n; (2) type: elementary, nodal, or ladder; (3) whether the embedding constant array represents an expansion in $\cos 2kq$ or $\cos(2k+1)q$ [cf. Eq. (2.11)]; (4) whether the roots are of odd order or even order; (5) orders v_L and v_R of the two roots; (6) array in which element c_m is the number of vertices exclusive of the roots of order $2m$; (7) number of elements in embedding constant array e_k; (8) greatest common factor f of the array elements e_k; and (9) pointer to another table giving location of the reduced array e_k/f. For ladder entries the following additional information is stored: (10) pointer to the same table giving location of the most recently added rung; and (11) the number of times l this particular rung is present in the ladder. The final piece of information is the weight w, which, because it is an integer of order $n!$, is stored in four 32-bit words as an IBM quadruple-precision real. All the remaining information is packed into additional sets of four 32-bit words.

This packing onto a fixed length of 32 bytes/entry considerably simplifies the data handling. The variable-length entries are restricted entirely to the table of reduced embedding constant arrays e_k/f, but it is a relatively short table and its handling is not a problem. Note also that packing leads in some cases to greater efficiency in the use of the data. For example, the entire array c_m fits in a single 32-bit word and the addition of two arrays c_m and c'_m becomes the addition of two single words. Since addition is the only operation performed on the c_m arrays in this particular program segment, those arrays need never be unpacked.

The rules for generating a new graph C from two graphs A and B are simple. A ladder C can be generated from all possible A and B that have the same information element 3, except that, to avoid overcounting, both may not simultaneously be ladders themselves. Also, again to avoid overcounting, the rungs are added in a particular order; if B is considered as the new rung to be added to A, it may not come from any table location beyond that of the previously added rung (see information element 10). If it comes from the same location, l is incremented by unity; otherwise, l is set equal unity (see information element 11). Then

$$
\begin{aligned}
n(C) &= n(A) + n(B) \\
v_{L,R}(C) &= v_{L,R}(A) + v_{L,R}(B) \\
c_m(C) &= c_m(A) + c_m(B) \\
e_k(C) &= e_k(A) \cdot e_k(B) \\
w(C) &= \binom{n(C)}{n(A)} w(A)\, w(B)/l
\end{aligned}
$$

The binomial coefficient in the expression for the new weight arises because of our decision to include a factor of $n!$ in (2.11); dividing the weight by l generates the correct $l!$ symmetry factor associated with l identical rungs in the ladder. Similarly, a nodal contribution C can be generated from all A and B that have the same information element 4, except that both may not be nodal. Now

$$n(C) = n(A) + n(B), \qquad v_L(C) = v_L(A), \qquad v_R(C) = v_R(B)$$

$$c_m(C) = c_m(A) + c_m(B) + \delta_{2m,\, v_R(A) + v_L(B)}$$

$$w(C) = \binom{n(C)}{n(A)} w(A)\, w(B)$$

The new embedding constant $e_k(C)$ is a convolution of the two arrays, $e_k(A)$ and $e_k(B)$; that is, the new array in Fourier space representation is a simple product of the old arrays.

As new contributions are generated, a search is initiated through the embedding constant array table for the reduced array e_k/f. If such an entry is found, the pointer to this old entry is recorded as information element 9; otherwise, a new entry is made and a new pointer is generated first. A search based on the B-tree algorithm described by Knuth[34] is then initiated through the table of ladder or nodal graphs. If an entry is found whose four 32-bit word descriptor is identical to the descriptor of the new contribution, the new weight w is added to the already stored weight. Otherwise, a new entry is established. Note that what is stored in this 2-rooted, 1-irreducible table of elementary, ladder, and nodal contributions is not necessarily individual graphs, but, rather, sums of graphs whose description elements 1–11 given above are the same. Even with this very significant packing, the cumulative number of entries in the table through order K^{21} is nearly 3,000,000 and requires three 40-megabyte tapes for storage.

We conclude by reviewing the most important features of the present calculation. First, it is not important that free embedding counts are larger than the counts in either the weak or the strong embedding scheme. What is crucial, and yet was not recognized in the Wortis article,[33] is that for the bcc family of lattices the free embedding count factorizes and each graph embedding constant reduces to a one-dimensional calculation. Also, each graph that contributes in dimension $d = 3$, say, also contributes in any other dimension d. Thus, the known $d = 1$ and $d = 2$ results serve as complete sum rule checks not available in the weak and strong embedding schemes. Second, although renormalization in the free embedding scheme replaces graphical complexity by algebraic complexity, it was recognized by

Wortis and co-workers[33, 35] that a significant advantage can still be gained by renormalization. That is, if the complete description of a graph as contained, say, in the adjacency matrix[33] is replaced by the limited algebraic information as given in 1–11 above, then many graphs may combine into a single algebraic entry. Savings in both handling time and storage increase dramatically with the order of the calculation.

At the 1-point and 2-point renormalization level used here, only elementary 2-rooted, 2-irreducible graphs need be generated and stored as graphs. For orders 7, 9, 11, 13, 15, 17, 19, and 21 the cumulative total number of elementary graphs required is approximately 1, 1, 6, 26, 145, 917, 6931, and 60,237. Extrapolation suggests that about 7×10^6 graphs would be required for an order-K^{25} calculation: such a list is quite manageable in terms of storage requirements. However, to generate this list is nontrivial by present techniques and will be discussed briefly in Section 5. We now believe this is a more fundamental barrier to any extension of the series for χ and M_2 than the problem of sorting and storing the 1-irreducible contributions as stated at Cargese.[9]

3. MODELS

The models discussed in this paper are distinguished by the scalar-field distribution function $f(\phi^2)$ in (2.1). In all our work below we choose the width of this distribution so that the second (cumulant) moment is unity; i.e.,

$$\mu_2 = \int d\phi\, \phi^2 f(\phi^2) \Big/ \int d\phi\, f(\phi^2) = 1 \tag{3.1}$$

With this normalization our definitions of certain models differ from the conventional ones by a rescaling of the inverse temperature parameter K.

3.1. Spin-S Ising Model

Of the many possible simple scalar models, probably the best known is the spin-S Ising model in which 3-dimensional quantum spins interact via the anisotropic coupling $JS_i^z S_j^z$. This model is equivalent to the scalar model (2.1) with the choice

$$f(\phi^2) = \sum_{m=-S}^{S} \delta(\phi + 2m\sqrt{y}), \qquad y = \frac{3}{4S(S+1)} \tag{3.2}$$

From the logarithmic derivative of the generating function (2.6) we easily derive

$$\mu_{2n} = \frac{d^{2n-1}}{dh^{2n-1}} \left[(2S+1)\sqrt{y}\coth[(2S+1)\sqrt{y}\,h] - \sqrt{y}\coth\sqrt{y}\,h \right]_{h=0} \tag{3.3}$$

which, by use of $(2S+1)^2 = 1 + 3/y$ and the known expansion for $\coth x$, we can also rewrite entirely in terms of the parameter y as

$$\mu_{2n} = [(3+y)^n - y^n] \frac{4^n B_{2n}}{2n} \tag{3.4}$$

where the B_{2n} are the Bernoulli numbers. Because of the particular polynomial form of the moments in (3.4), the expressions (1.1) and (1.2) for χ and M_2 reduce to the double power series of essentially triangular form

$$\chi(K, y) = A_0^0 + \sum_{n=1} K^n \sum_{m=1}^{n} \frac{A_n^m}{m!} y^{m-1}$$

$$M_2(K, y) = \sum_{n=1} K^n \sum_{m=1}^{n} \frac{B_n^m}{m!} y^{m-1} \tag{3.5}$$

Because the coefficients A_n^m and B_n^m for the spin-S models are not integers (though they could be expressed as rational fractions), they will not be presented here. Readers interested in these tables should consult the authors. However, the single variable series for $S = 1/2$, 1, 2, and ∞ in dimensions 2 and 3 are given in the Appendix (Table I).

3.2. Blume–Capel Model

Another simple model that has been discussed in the literature and is useful for the study of tricritical behavior in addition to ordinary critical behavior is the Blume–Capel, or 3-state, model.[25] The distribution function with our normalization (3.1) is

$$f(\phi^2) = \delta(\phi + \sqrt{y}) + 2(y-1)\,\delta(\phi) + \delta(\phi - \sqrt{y}) \tag{3.6}$$

and its cumulant moments are given by

$$\mu_{2n} = \frac{d^{2n-1}}{dh^{2n-1}} \left[\frac{\sqrt{y}\sinh\sqrt{y}\,h}{y - 1 + \cosh\sqrt{y}\,h} \right]_{h=0} \tag{3.7}$$

Explicit power series division in (3.7) shows that the μ_{2n} for $n>1$ can be generated recursively from the relation

$$\mu_{2n} = y^{n-1} - \sum_{m=1}^{n-1} y^{n-1-m} \binom{2n-1}{2m-1} \mu_{2m} \tag{3.8}$$

Because the μ_{2n} in (3.8) are of the same polynomial form as in (3.4), the Blume–Capel χ and M_2 series are also expressible in the triangular form (3.5). The coefficients A_n^m and B_n^m for this model in both $d=2$ and $d=3$ are listed in the Appendix (Table II). Except for the $A_0^0=1$ entry in the tables for χ, m varies from 1 to n for fixed n in each block of n values. Two checks are possible in that $y=1$ is the $S=1/2$ model, $y=3/2$ is $S=1$. The value $y=2$ yields the $l=2$ "loop model" mentioned most recently by Zinn-Justin.[7] In the neighborhood of some critical value $K=K_t(y)$, $y=y_t>2$, the model is expected to display tricritical behavior. In the future one might attempt both to locate this point and deduce the expected logarithmic corrections that modify the classical (mean field) behavior in $d=3$. However for the present we believe it is more useful to deal with simpler models in which the mean-field point is purely Gaussian and its location is exactly known.

3.3. Ising-Gaussian Interpolation Models

One simple model that can interpolate between $S=1/2$ Ising and Gaussian behavior is a model of classical, fixed-length, y-dimensional spins, again coupled anisotropically via $JS_i^z S_j^z$. In this case the equivalent scalar distribution is

$$f(\phi^2) = \begin{cases} (y-\phi^2)^{(y-3)/2}, & |\phi| < \sqrt{y} \\ 0, & |\phi| > \sqrt{y} \end{cases} \tag{3.9}$$

which in the limit $y \to 1$ becomes the $S=1/2$ Ising distribution and in the limit $y \to \infty$ becomes the Gaussian $f \propto \exp(-\phi^2/2)$. In the interval $1<y<\infty$, the model passes through the $S=\infty$ Ising point at $y=3$. However, the power moments of the distribution, $m_{2n} \equiv \int f(\phi^2)\phi^{2n}\, d\phi$, which can be determined recursively from

$$m_{2n+2} = \frac{y(2n+1)}{y+2n} m_{2n} \tag{3.10}$$

are not polynomials in y and thus a simple triangular expansion as in (3.5) is not possible. Similarly, the ϕ^4 model[1] defined by $f(\phi^2) \propto \exp[\alpha\phi^2 - \beta(\alpha)\phi^4]$, $\beta(\alpha)>0$, does not have a triangular expansion.

We have not bothered to tabulate single variable series for these models, but have instead concentrated on two other models which do have triangular expansions similar to (3.5). These models, the Klauder[26] and double-Gaussian,[23] or range,[27] also allow interpolation between $S=1/2$ Ising and Gaussian. A possible limitation is that they are not defined for temperatures below some critical value, i.e., $K>K^*(y)$. However, as this temperature is below the interesting second-order phase transition line $K=K_c(y)$, we feel they are useful nonetheless and hope that our work will trigger further investigations into their properties.

3.4. Klauder Model

The Klauder model[26] is defined by the distribution

$$f(\phi^2)=|\phi|^{y/(1-y)}\, e^{-\phi^2/2(1-y)} \tag{3.11}$$

provided that

$$K<K^*(y)=\frac{1}{2^d(1-y)} \tag{3.12}$$

On the interval $0\leqslant y\leqslant 1$ the model interpolates between Gaussian and $S=1/2$ Ising. Since the moments satisfy the recursion relations

$$m_{2n+2}=(2n+1-2ny)m_{2n} \tag{3.13}$$

the cumulant moments μ_{2n} are again polynomials of order $n-1$ as in (3.4). It is, however, convenient to rewrite the expansion for χ and M_2 for the model as

$$\begin{aligned}\chi(K, y)&=A_0^0+\sum_{n=1}\frac{2^n}{n!}K^n\sum_{m=1}^{n}A_n^m\, y^{m-1}\\ M_2(K, y)&=\sum_{n=1}\frac{2^n}{n!}K^n\sum_{m=1}^{n}B_n^m\, y^{m-1}\end{aligned} \tag{3.14}$$

For $d=3$ the coefficients A_n^m and B_n^m are integers and are listed in Table III of the Appendix with precisely the same ordering as used for the Blume–Capel model series.

Some properties of the Klauder model in the vicinity of the Gaussian line $y=0$ can be determined fairly directly, as we illustrate below specifically for $d=3$. Note that at $y=0$ all μ_{2n} for $n>1$ vanish and the propagator (2.3) is given by the free-field expression

$$G_0(\mathbf{q}, K)=(1-8K\cos q_x\cos q_y\cos q_z)^{-1} \tag{3.15}$$

Corrections to this result can be derived systematically if we treat y as a small parameter. To obtain a complete description near the critical point the full machinery of renormalized perturbation theory should be used, but here we will only evaluate the leading y dependence of the critical line $K_c(y)$, for which lowest order elementary perturbation theory is adequate. For small y the cumulant moments are given by

$$\mu_{2n+2} \approx (-2)^n n!\, y, \qquad n \geqslant 0 \tag{3.16}$$

Then the propagator to leading order in y is modified by a self-energy which is a sum of terms, each corresponding to a single vertex insert of order greater than two. Attached to the vertex of order $2n+2$ are n closed loops with symmetry factor $2^n n!$. Each loop contributes a factor given by the momentum integral

$$I(K) = \int \frac{d^3q}{(2\pi)^3} [G_0(\mathbf{q}, K) - 1] \tag{3.17}$$

and so the complete self-energy contribution is

$$\sum_{n=1}^{\infty} \frac{\mu_{2n+2}}{2^n n!} [I(K)]^n = -\frac{yI(K)}{1+I(K)} \tag{3.18}$$

The susceptibility is

$$G(\mathbf{q}, K) \approx \left(1 - 8K \cos q_x \cos q_y \cos q_z + \frac{yI(K)}{1+I(K)}\right)^{-1} \tag{3.19}$$

and the critical $K_c(y)$ is determined by the divergence of $G(0, K)$. To leading order in y,

$$8K_c(y) \approx 1 + \frac{yI(1/8)}{1+I(1/8)} \tag{3.20}$$

Numerically, $I(1/8) = (4/\pi^2)\, K^2(1/2) - 1 \approx 0.3982...$, where here $K(m)$ is the complete elliptic integral.[36] Note that the instability line as given by (3.12) is, to leading order in y,

$$8K^*(y) \approx 1 + y \tag{3.21}$$

and thus for $y > 0$, $K_c < K^*$. For $y < 0$, $K_c > K^*$ and Ising-like critical behavior *cannot* be observed in this regime. It is for this reason that we believe the model is not useful for the purpose originally envisioned by Klauder.[26]

3.5. Double-Gaussian Model

The second very useful model with a triangular expansion is the double-Gaussian model defined by

$$f(\phi^2) = \exp\left[-\frac{(\phi+\sqrt{y})^2}{2(1-y)}\right] + \exp\left[-\frac{(\phi-\sqrt{y})^2}{2(1-y)}\right] \tag{3.22}$$

provided the restriction (3.12) is again fulfilled. Also,[7] just as for the Klauder model, this model interpolates between Gaussian and $S=1/2$ Ising as y varies between 0 and 1. However, somewhat surprisingly, this model has an analytic continuation to the regime $y>1$, which can be interpreted physically and which we call the range model. The cumulant moments for the double-Gaussian model are simply related to the $S=1/2$ Ising moments $\mu_{2n}^{(I)} = (4^n-1)4^n B_{2n}/(2n)$, given in (3.4),

$$\mu_{2n} = \begin{cases} \mu_2^{(I)} = 1, & n=1 \\ y^n \mu_{2n}^{(I)}, & n>1 \end{cases} \tag{3.23}$$

and the expressions (1.1) and (1.2) for χ and M_2 can therefore be written

$$\begin{aligned} \chi(K, y) &= A_0^0 + \sum_{n=1} K^n \left(A_n^0 + \sum_{m=1}^{n} \frac{A_n^m}{m!} y^{m+1} \right) \\ M_2(K, y) &= \sum_{n=1} K^n \left(B_n^0 + \sum_{m=1}^{n} \frac{B_n^m}{m!} y^{m+1} \right) \end{aligned} \tag{3.24}$$

The integer coefficients A_n^m and B_n^m are listed in Table IV of the Appendix for $d=3$. Within each block of $n+1$ entries, m varies from 0 to n. Note that a 3-way sum rule check is possible between Blume–Capel, Klauder, and double-Gaussian tables by setting $y=1$.

An analysis similar to that described for the Klauder model can be used to determine the leading behavior of the critical line $K_c(y)$. In this case, (3.23) shows directly that the leading self-energy corrections involve only the fourth-order vertex insert at order y^2 and the sixth-order vertex insert at order y^3. We find

$$G(\mathbf{q}, K) \approx \{1 - 8K \cos q_x \cos q_y \cos q_z + y^2 I(K) - 2y^3 [I(K)]^2\}^{-1} \tag{3.25}$$

[7] One can show that both models are members of a class of one-parameter models with triangular expansions for the series coefficients, all of which interpolate continuously between Ising and Gaussian limits. The moment generating functions $G(h) = \int f(\phi^2) \exp(-h\phi)\, d\phi$ for this class satisfy the second-order differential equation $G'' - (1+\lambda)(1-y)hG' - [1-\lambda(1-y)^2 h^2]G = 0$, with $0 \leqslant \lambda \leqslant 1$. The value $\lambda = 0$ corresponds to the Klauder model and $\lambda = 1$ to the double-Gaussian model.

which diverges at $\mathbf{q}=0$ when $K=K_c(y)$, where

$$8K_c(y) \approx 1 + y^2 I(\tfrac{1}{8}) - 2y^3 [I(\tfrac{1}{8})]^2 \tag{3.26}$$

Again, for $y>0$, $K_c<K^*$, and so it is consistent to identify $K_c(y)$ as the critical line.

3.6. Range Model

As observed by Baker and Bishop,[27] the partition function (2.1) in uniform magnetic field $h_i=h$ with the double-Gaussian distribution (3.22) can be written in the Ising-like form of a sum over discrete "spin" values:

$$Z_{\mathrm{DG}}(K, y, h) = \sum_{\{s_i=\pm 1\}} \prod_i \int d\phi_i \exp\left\{ K \sum_{nn} \phi_i \phi_j - \sum_i \frac{(\phi_i - s_i\sqrt{y})^2}{2(1-y)} + h \sum_i \phi_i \right\} \tag{3.27}$$

or

$$Z_{\mathrm{DG}}(K, y, h) = Z_1(y) \sum_{\{s_i=\pm 1\}} \prod_i \int d\phi_i \exp\left\{ -\frac{1}{2} \sum_{ij} \phi_i M_{ij} \phi_j + \sum_i \phi_i \left(h + \frac{s_i\sqrt{y}}{1-y} \right) \right\} \tag{3.28}$$

where

$$M_{ij} = \int \frac{d^d q}{(2\pi)^d} M_{\mathbf{q}} \exp[i\mathbf{q}\cdot(\mathbf{r}_i - \mathbf{r}_j)], \qquad M_{\mathbf{q}} = \frac{1}{1-y} - KV_{\mathbf{q}} \tag{3.29}$$

with $V_{\mathbf{q}}$ the "nearest" neighbor interaction (2.8). The prefactor $Z_1(y)$ in (3.28) does not depend on the field h and hence will not enter into the calculation of the susceptibility to be discussed below. The integration over the Gaussian field variables ϕ_i is accomplished by first shifting ϕ_i to $\phi_i + \sum_j M_{ij}^{-1}[h + s_j y^{1/2}/(1-y)]$, where the inverse matrix M_{ij}^{-1} is

$$\begin{aligned} M_{ij}^{-1} &= \int \frac{d^d q}{(2\pi)^d} M_{\mathbf{q}}^{-1} \{\exp[i\mathbf{q}\cdot(\mathbf{r}_i - \mathbf{r}_j)]\} \\ &= (1-y)\,\delta_{ij} + K(1-y)^2 \\ &\quad \times \int \frac{d^d q}{(2\pi)^d} \frac{V_{\mathbf{q}}}{1 - K(1-y)V_{\mathbf{q}}} \exp[i\mathbf{q}\cdot(\mathbf{r}_i - \mathbf{r}_j)] \end{aligned} \tag{3.30}$$

We obtain

$$Z_{\mathrm{DG}}(K, y, h) = Z_2 \sum_{\{s_i = \pm 1\}} \exp\left\{\frac{1}{2}\sum_{ij}\left(h + \frac{s_i\sqrt{y}}{1-y}\right) \times M_{ij}^{-1}\left(h + \frac{s_i\sqrt{y}}{1-y}\right)\right\} \tag{3.31}$$

and the argument of the exponential in (3.31) can be simplified, with the use of the result $\sum_j M_{ij}^{-1} = (1-y)/[1-2^d K(1-y)]$, to

$$\left\{\frac{y}{2(1-y)^2}\sum_{ij} s_i M_{ij}^{-1} s_j + h\sqrt{y}\sum_i \frac{s_i}{1-2^d K(1-y)} + \frac{1}{2}\frac{Nh^2(1-y)}{1+2^d K(1-y)}\right\} \tag{3.32}$$

where N is the number of sites in the lattice. Note also that the diagonal term $(1-y)\,\delta_{ij}$ in (3.30) will contribute a constant to the quadratic $s_i M_{ij}^{-1} s_j$, which can be absorbed into the prefactor in (3.31) and change it to $Z_3(K, y)$.

Let us now define an $S = 1/2$ Ising model with the "long"-range interaction $K' J_{ij}(\rho)$, where

$$J_{ij}(\rho) = \int \frac{d^d q}{(2\pi)^d} \frac{V_{\mathbf{q}}}{1-\rho V_{\mathbf{q}}} \exp[i\mathbf{q}\cdot(\mathbf{r}_i - \mathbf{r}_j)] \tag{3.33}$$

Provided $|\rho| < 2^{-d}$, the interactions are exponentially damped with distance; in the coordinate direction x, say, $J_{ij} \sim e^{-x_{ij}/\lambda}$, where the range λ is the solution of $\cosh(1/\lambda) = 2^{-d}/|\rho|$. For $K' > 0$, which we consider here, the "nearest" neighbor interaction is always ferromagnetic, as indeed are all interactions between a spin at the origin and a spin on the odd lattice sites $(2l+1, 2m+1, \ldots)$. However, the interactions between spins at the origin and even lattice sites $(2l, 2m, \ldots)$ are only ferromagnetic for $\rho > 0$; for $\rho < 0$ these interactions inhibit ferromagnetic ordering. But since the total interaction $\sum_j J_{ij} = 2^d/(1-2^d\rho)$ is always ferromagnetic, the model is only an example of a *partially frustrated* ferromagnet in the regime $\rho < 0$. The partition function for this model, which we call the range model, is defined as

$$Z_{\mathrm{R}}(K', \rho, h') = \sum_{\{s_i = \pm 1\}} \exp\left\{\frac{1}{2}K'\sum_{ij} s_i J_{ij}(\rho) s_j + h'\sum_i s_i\right\} \tag{3.34}$$

and on comparing (3.34) with (3.31) and (3.32) we find

$$\ln Z_{\mathrm{DG}}(K, y, h) = \ln Z_{\mathrm{R}}(Ky, K(1-y), \sqrt{y}\,h/[1-2^d K(1-y)]) + \tfrac{1}{2}Nh^2(1-y)/[1-2^d K(1-y)] + \ln Z_3(K, y) \tag{3.35}$$

That is, except for some trivial additive functions, the double-Gaussian and range model free energies are equal, provided we make the parameter identifications

$$K' = Ky, \qquad \rho = K(1-y), \qquad h' = \frac{\sqrt{y}\, h}{1 - 2^d K(1-y)} \tag{3.36}$$

By differentiating (3.35) twice with respect to field, we find

$$\chi_{DG} = \frac{y}{[1-2^d K(1-y)]^2}\chi_R + \frac{1-y}{1-2^d K(1-y)} \tag{3.37}$$

which implies that χ_R has the expansion

$$\chi_R(K, y) = 1 + \sum_{n=1} K^n \sum_{m=1}^{n} \frac{R_n^m}{m!} y^m \tag{3.38}$$

The coefficients R_n^m are given in terms of the coefficients A_n^m of the double-Gaussian expansion (3.24) by

$$\begin{aligned} R_n^m = {} & 2^{dn}\delta_{m1} + A_n^m - 2^{d+1}(A_{n-1}^m - mA_{n-1}^{m-1}) \\ & + 2^{2d}[A_{n-2}^m - 2mA_{n-2}^{m-1} + m(m-1)A_{n-2}^{m-2}] \end{aligned} \tag{3.39}$$

with the proviso that the A_l^k on the right-hand side are set to zero whenever $l<1$ or $k<1$ or $k>l$.

As stressed above, the range model analytically continues the double-Gaussian model to the region $y>1$ provided that $(y-1)K<2^{-d}$. No analysis of the series (3.38) have been performed to date, but an estimate of the critical line $K_c(y)$ has been obtained for $d=3$ by a crude least-squares fit to double-Gaussian model approximants in the range $0.5 < y \leqslant 1$. Our approximation is

$$K_c^{-1}(y) \approx 8 - 3.05602y^2 + 2.96137y^3 - 2.5771y^4 + 1.274y^5 - 0.248y^6 \tag{3.40}$$

The coefficients of y^2 and y^3 were not fixed in the fit and yet are within 4% and 14%, respectively of the exact values given in (3.26). The estimate (3.40) intersects the model boundary $K^{-1} = 8(y-1)$ at $y \approx 1.6$, and thus critical behavior over the wide range $1 < y \leqslant 1.6$ remains to be explored by single-variable series analysis. On the other hand, since Chen *et al.*[13] could clearly identify only a single Ising-like multicritical point in the range $0 < y < 1.8$ for the double-Gaussian model, universality of critical exponents is to be expected.

4. DOUBLE-GAUSSIAN SERIES ANALYSIS

The analysis described in this section is based on the method of confluent inhomogeneous second-order differential equations discussed by Rehr *et al.*[28] Its utility lies in the fact that it may lead to a significant test of the universality hypothesis. As discussed in Sec. 1, the method biases the unknown functions of interest to have the appropriate leading critical behavior (1.4) which, although not of the scaling form discussed by Wegner,[30] should be adequate, provided higher order terms in $(K_c - K)^{n\theta}$ and other corrections proportional to $(K_c - K)^{\theta_n}$, $\theta_n > \theta$, are small or can be incorporated into the analytical factors $A_F(K)$ and $a_F(K)$ or an "effective" background $B_F(K)$.

We have analyzed in detail the three-dimensional double-Gaussian model discussed in Sec. 3, which we believe is typical of models that interpolate between spin-1/2 Ising and Gaussian limits. Of course, we investigate the model only at a discrete set of parameter values. These are chosen so that the width of each Gaussian in the distribution (3.22) is an integer multiple of 0.05, i.e.,

$$\omega \equiv \sqrt{1-y} = 0.05n \tag{4.1}$$

We could only successfully determine approximants with the critical behavior (1.4) in the range $0 \leqslant \omega \leqslant 0.70$; presumably for larger ω the higher order terms $(K_c - K)^{n\theta}$ or other confluent corrections are so large that the fact that (1.4) is not of scaling form is significant. If $\theta = 0.5$ exactly, (1.4) would *in principle* contain such terms. Also, because the double exponential fitting problem is so unstable, we limited ourselves to the biased problem in which $\theta_F = \theta$ is fixed in (1.4). If a common θ can be found for which the γ_F are independent of ω, then, in a limited sense, we will have verified one aspect of universality.

The approximations to χ, M_2, and $\xi^2 \propto M_2/\chi$ which have the confluent asymptotic critical behavior (1.4) are determined as the solutions of the second-order differential equation

$$[Q_2(K)\, D_2 + Q_1(K)\, D_1 + Q_0(K)]\, F(K) = P(K) \tag{4.2}$$

where the $Q_i(K)$ and $P(K)$ are polynomials in K with $Q_1(K)$ and $Q_2(K)$ forced to take the factorizable form

$$Q_1(K) = (K_c - K)\, \dot{Q}_1(K) \qquad Q_2(K) = (K_c - K)^2\, (K_c + K)\, \dot{Q}_2(K) \tag{4.3}$$

The D_i in Eq. (4.2) are differential operators in K of order i, and the coefficients in the polynomials $Q_i(K)$ and $P(K)$ are fit so that (4.2) is satisfied

as a power series to some order K^N. In addition to the Rehr *et al.*[28] choice for the differential operators

$$D_1 = K\frac{d}{dK} \qquad D_2 = D_1^2 \tag{4.4}$$

we have used others, such as

$$D_1 = \frac{d}{dK} \qquad D_2 = \begin{cases} D_1^2 \\ K D_1^2 \end{cases} \tag{4.5}$$

Finally, we have restricted our choice of approximants to those in which the degrees of the $Q_i(K)$ are roughly comparable. The essential difference between our differential approximants and those of Guttmann[20] is the inclusion of the constraints in Eq. (4.3). Without these constraints, the solution of Eq. (4.2) generally consists of a single power-law singularity together with analytic factors and background terms, i.e., a solution which ignores non-analytic confluent singularities.

The numerical procedure for determining the critical constants in (1.4) is straightforward. For fixed K_c in (4.3) the remaining coefficients in Q_i and P are obtained from the solution of a set of linear equations. Solutions in which the function $\hat{Q}_2(K)$ has zeros in the disk $|K| < K_c$ or near K_c are considered "defective" and ignored. Knowledge of the polynomials $Q_i(K)$ suffices to determine γ_F and θ_F directly as the solutions of a quadratic indicial equation.[28] As already observed for the spin-S Ising model,[9] very reproducible correlations between γ_F and θ_F are found as K_c is varied. To fix $\theta_F = \theta$ and hence determine our *biased* γ_F estimates, we employ a Newton–Raphson search which starts with K_c near the critical line given by (3.40). Occasionally, no real solution to this nonlinear problem can be found. For θ in the neighborhood of 0.5 most final estimates of K_c at order K^{21} lie within 5×10^{-6} of the value (3.40) for $0 \leqslant \omega \leqslant 0.70$. The dispersion in these estimates is much smaller at about $\pm 2 \times 10^{-6}$. The use of several different choices of differential operators D_i has proved to be important. For reasons we do not understand, for some parameter ranges many approximants can be found for some particular choices of D_i, but not for others. The amplitudes A_F and a_F in (1.4) can be obtained by integrating the differential equation (4.2) numerically, starting with the known initial conditions at $K = 0$. A simpler and faster procedure,[28] which we have adopted here, is to use the differential equation (4.2) to generate two power series representations of $F(K)$, one about $K = 0$, the other about $K = K_c$. The expansion about $K = 0$ agrees with the known series through the order used (e.g., 21) and thereafter simply extends this series to higher order, while the expansion about $K = K_c$ depends linearly on the two unknown

amplitudes A_F and $A_F a_F$. These series can be used directly to evaluate the function in the interval $0 < K < K_c$ and matching F and dF/dK at some conveniently chosen intermediate K then determines A_F and a_F.

We have included in Table V of the Appendix 50-term series obtained from two representative differential approximants to the 21-term spin-1/2 Ising model susceptibility series: $xd/dx[9, 6, 9; \phi]$ and $d/dx[7, 6, 7; 1]$. We hope these series will prove useful in tests of other methods of confluent singularity analysis. The series coefficients satisfy 9-term recurrence rela-

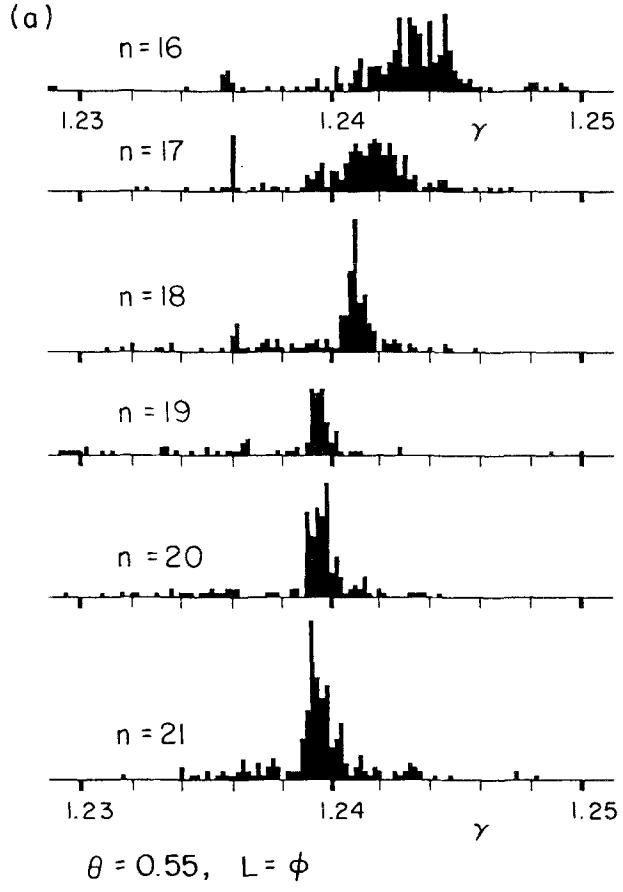

Fig. 2. (a) Number of homogeneous approximants to $\chi(\omega)$ yielding a particular γ with a resolution 2×10^{-4}, with a fixed correction-to-scaling exponent $\theta = 0.55$. Results, cumulative over $\omega = 0, 0.05, \ldots, 0.70$, show overall convergence with order; (b) As in (a), but showing instead estimates of $1 - \alpha$ within a resolution 2×10^{-3} from the antiferromagnetic singularity in χ; (c) Again, estimates of γ from χ. Here $\theta = 0.50$ and $n = 21$ are fixed. The order of the inhomogeneous term P_L in (4.2) varies from $L = \phi$ (P_L null) through $L = 2$ as indicated.

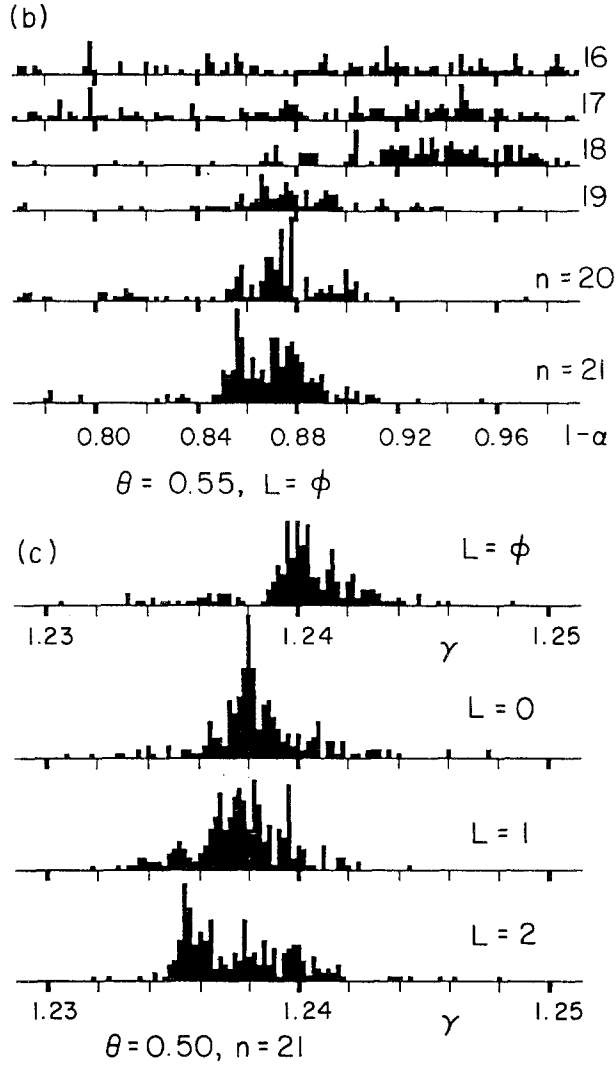

Fig. 2. (*Continued*)

tions of the form $\sum_{ij} Q(i, j)(n-j)^i c(n-j) = P(n)$, from which additional terms can be calculated.

Two important trends are apparent when all the data for $0 \leqslant \omega \leqslant 0.70$ are combined into a single output. The first is convergence with order; in Figs. 2a and 2b we show histograms of the number of biased *homogeneous* ($L = \phi$) differential approximant estimates for γ and $1-\alpha$ with $\theta = 0.55$

based on χ series to order K^n, $n = 16, 17, \ldots, 21$. We note that even forcing a correction-to-scaling term, as we have done by using (4.2), does not guarantee converged estimates if the series length is too short. Consistency suggests that only the $n = 19$, 20, and 21 estimates for γ represent the asymptotic value. It is interesting but probably coincidental that also no significant estimate of $1 - \alpha$ can be made until $n \geqslant 19$. The second important trend results from allowing for a nonvanishing polynomial $P(K)$ in (4.2). In Fig. 2c we show biased estimates γ with $\theta = 0.50$, with P ranging from null ($L = \phi$) to finite order $L = 0$, 1, 2. There is a significant drop in the estimate of γ in going from $L = \phi$ to 0 or 1, while at $l = 2$ the dispersion in the estimates begins to increase. Since we have no *a priori* reason for believing the background B_F in (1.4) should be zero and hence P null, and because they tend to reduce the scatter and improve overall consistency, we base most of our quantitative estimates in the following on $L = 1$ inhomogeneous differential approximants.

Detailed results explicitly showing variations with ω are displayed in Figs. 3–6. Figures 3 and 4 are histograms of the number of biased estimates of γ for each value of ω separately; Fig. 3 illustrates convergence with order, while Fig. 4 illustrates the effect of inhomogeneous terms in the differential equation (4.2). In both figures we also show the effect of changes in θ between 0.50 and 0.55 at order K^{21}. We find that γ correlates positively with θ for small ω and anticorrelates with θ for large ω, in qualitative agreement with the spin-S Ising results.[9] Our "best" approximants are those obtained with the polynomial P of order $L = 1$; those based on the operator choice (4.5) are shown in Figs. 4c and 4d for $\theta = 0.50$ and 0.55. From this and additional data based on the choice (4.4) we conclude that universality is best satisfied with

$$\gamma = 1.237 \pm 0.002, \qquad \theta_\chi = 0.52 \pm 0.03 \tag{4.6}$$

The error bars are subjective, but, we believe, reasonable. In particular, the very distinct downward trend of γ with increasing ω shown in Fig. 4d makes any value $\theta > 0.55$ unreasonable if universality is assumed. On the other hand, θ slightly smaller than 0.50 is probably not excluded by the data shown in Fig. 4c, especially if the estimates for $\omega \geqslant 0.60$ are excluded as unreliable. Such exclusion might be reasonable, since the amplitude a_χ is large in this regime and the form (1.4) is likely first to become inadequate there. Finally, the estimate (4.6) is lower than our preliminary spin-S estimate $\gamma = 1.239 \pm 0.002$ almost certainly because of our present reliance on inhomogeneous approximants. Figure 5 shows histograms of biased estimates of 2ν determined from $M_2/\chi = 2\xi^2$ approximants. Again, from the

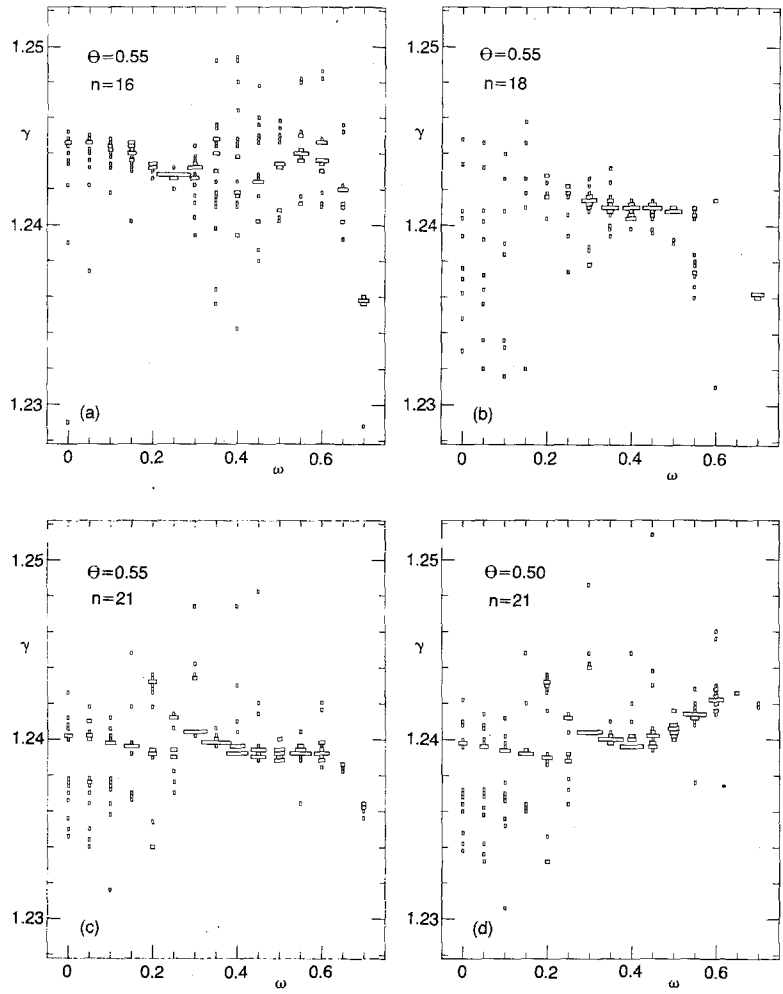

Fig. 3. Histograms, centered on discrete ω, of the number of homogeneous approximants to $\chi(\omega)$ yielding a particular γ with resolution 2×10^{-4}. For each ω, about 25 approximants with the choice (4.5) are sought; of those that are found, only the nondefective are plotted. This number may be small, as, for example, in (b), where for $\omega = 0, 0.05, \ldots$ only 10, 10, 8, 6, 7,... estimates are available. Plots (a), (b), and (c) show variations with order n with fixed $\theta = 0.55$ and are a detailed breakdown of some of the cumulative results in Fig. 2a. The result of changing to $\theta = 0.50$ with $n = 21$ is shown in (*d*). The equivalent cumulative result is shown in Fig. 2c.

$L=1$ data shown in Figs. 5c and 5d and from additional data based on (4.4), we conclude that universality is best satisfied with

$$2\nu = 1.260 \pm 0.003, \qquad \theta_{\xi^2} = 0.51 \pm 0.03 \tag{4.7}$$

The consistency between θ_{ξ^2} and θ_χ is noteworthy.

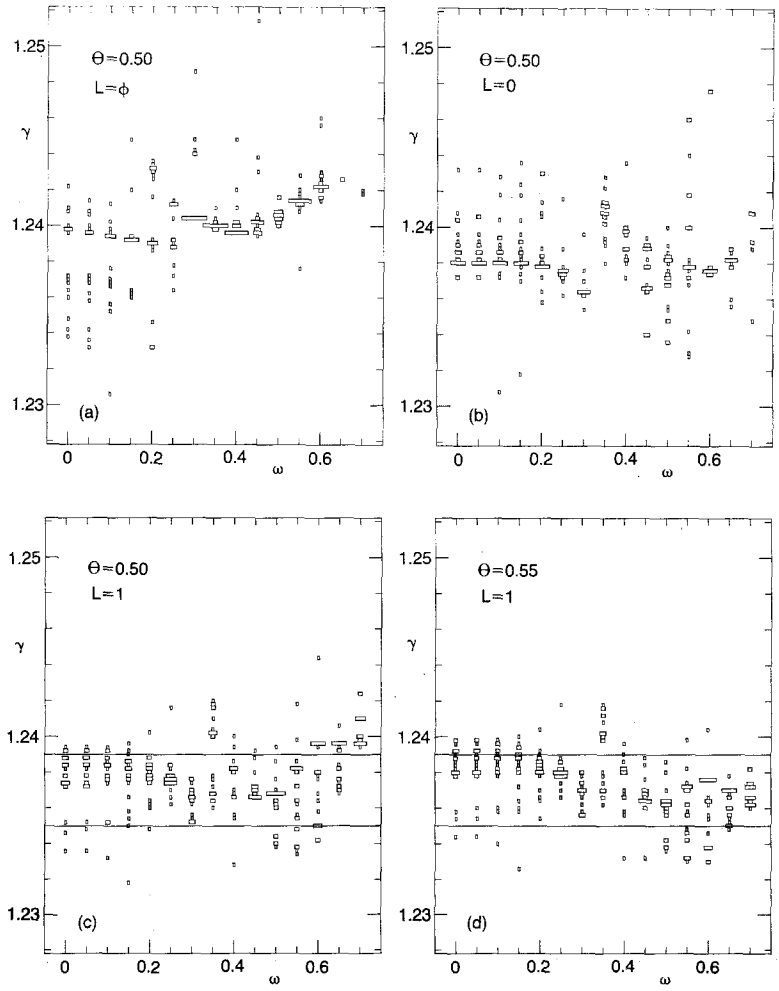

Fig. 4. Histograms of γ estimates similar to Fig. 3, but with $n=21$ fixed and a possible inhomogeneous term P_L in (4.2). Plots (a), (b), and (c) show variation with order L with fixed $\theta=0.50$ and are a detailed breakdown of some cumulative results in Fig. 2c. The result of changing to $\theta=0.55$ with $L=1$ is shown in (d). The solid horizontal lines in (c) and (d) indicate the bounds in our estimate $\gamma=1.237\pm0.002$.

Finally, Fig. 6 shows histograms of $1-\alpha$ based on both χ and M_2/χ series. A correction-to-scaling term is *not* built into the antiferromagnetic singular point in (1.4) and hence the substantial deviations from universal behavior are not surprising. From the low-ω regime we conclude that

$$\alpha = 0.11 \pm 0.02 \tag{4.8}$$

which agrees with the value given by the hyperscaling relation, $\alpha = 2 - 3\nu$, using the estimate (4.7); however, the precision is not sufficient for a

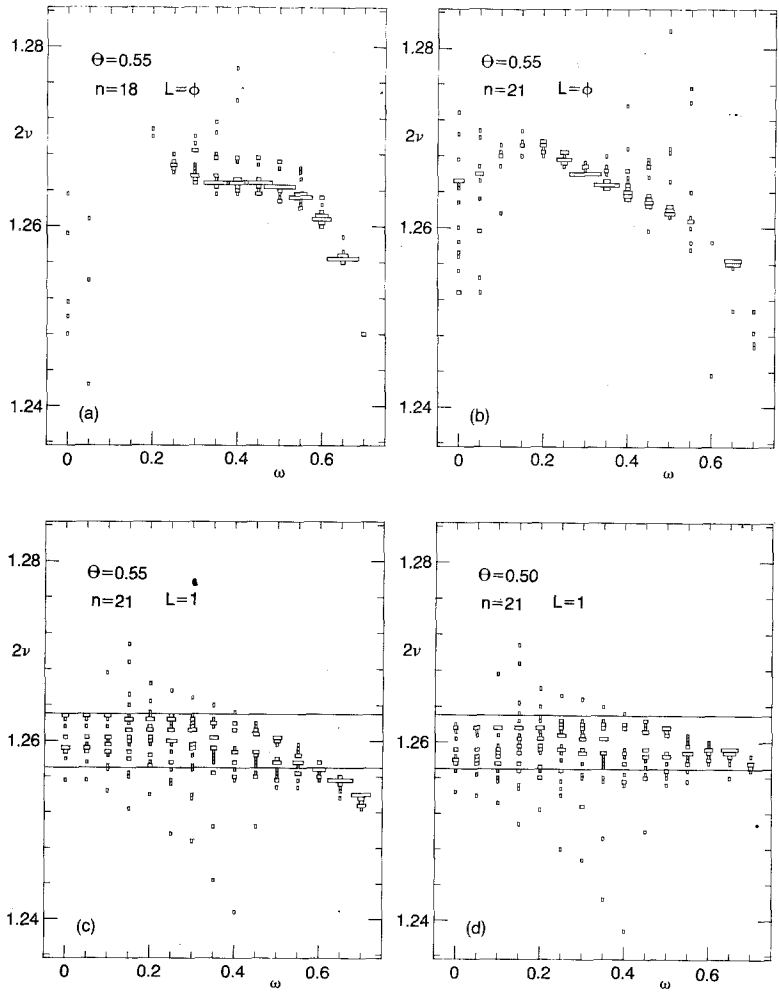

Fig. 5. Histograms of 2ν estimates based on approximants to ξ^2 with the choice (4.5). Plots (a)–(d) show variations with n, L, and θ as labeled. Resolution in 2ν is 4×10^{-4}. The solid horizontal lines in (c) and (d) indicate the bounds in our estimate $2\nu = 1.260 \pm 0.003$.

definitive test. At the particular value $\omega = 0.31$ (i.e., $y^* = 0.90$) our approximants yield $1 - \alpha_\chi = 0.895 \pm 0.01$, in good agreement with the estimate of ref. 19. While the hyperscaling relation $\alpha = 2 - 3\nu$ is satisfied better at this value of ω, drawing conclusions about the validity of hyperscaling based on a single series estimate may be misleading.

From (4.6) and (4.7) we deduce $\eta = 2 - \gamma/\nu = 0.036 \pm 0.006$, if we assume that the errors in γ and ν are uncorrelated. However, this is not

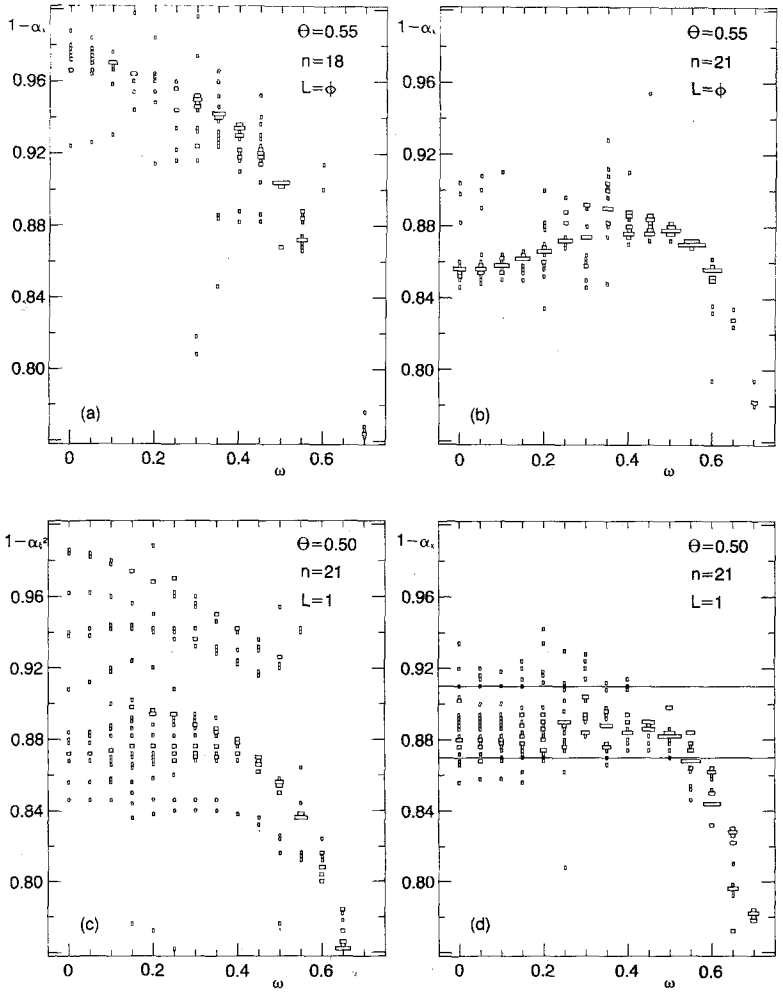

Fig. 6. Histograms of $1 - \alpha$ estimates from χ or ξ^2 series as labeled. Resolution in $1 - \alpha$ is 2×10^{-3}. Plots (a) and (b) are a detailed breakdown of some cumulative results shown in Fig. 2b. The solid horizontal lines in (d) indicate the bounds in our estimate $\alpha = 0.11 \pm 0.02$.

realistic, since we observe strong linear correlation with nearly equal slopes between the pairs γ and K_c, and 2ν and K_c. If we impose the obvious constraint that χ and M_2/χ have the same K_c, we find $2\nu - \gamma = 0.0226 \pm 0.0004$ and hence

$$\eta = 0.0359 \pm 0.0007 \tag{4.9}$$

This value is consistent with the latest field-theoretic results from ref. 4, $\eta \approx 0.0365 \pm 0.003$, and marginally consistent with the series estimate from ref. 18, $\eta \approx 0.0375(10)$ (again doubling those authors' one-standard-deviation error estimates). Note that our best estimates of γ and 2ν in Eqs. (4.6) and (4.7) are also consistent with this constraint on K_c; with $\gamma = 1.237$ we obtain $2\nu = 1.2596 \pm 0.0004$; and with $2\nu = 1.260$ we obtain $\gamma = 1.2374 \pm 0.004$.

Precise and meaningful values for the correction-to-scaling amplitudes cannot be given without first specifying the critical exponents. We show in Figs. 7a and 7b the very nearly linear correlations between a_χ and γ, and

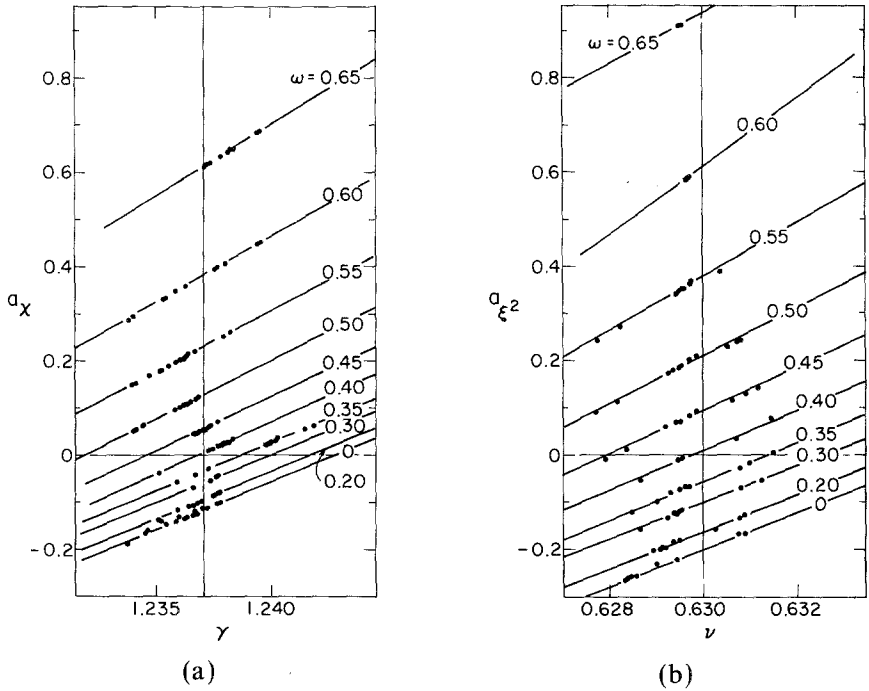

Fig. 7. Correction-to-scaling amplitudes. (a) Correlation plot a_χ versus γ from χ approximants with the choice (4.4) and $\theta = 0.50$; (b) correlation plot of a_{ξ^2} versus 2ν from ξ^2 approximants with the choice (4.4) and $\theta = 0.50$.

a_{ξ^2} and 2ν, obtained from our inhomogeneous approximants with $L=1$ and $\theta=0.50$. Thus, with the central values in (4.6) and (4.7) we find that the leading correction to scaling vanishes consistently for χ and M_2/χ at $\omega=\omega^*$, $y=y^*$ with

$$\omega^*=0.39, \qquad y^*=0.85 \tag{4.10}$$

With the Chen *et al.*[13] central estimate of $y^*=0.87$ we obtain from Fig. 7 the value $\gamma\approx 1.2383$, consistent with their result (1.2385), and predict $\nu\approx 0.6311$. Similarly, with $y^*=0.90$ of ref. 19, we obtain $\gamma\approx 1.2395$ and $\nu\approx 0.6322$, which are again consistent with their estimates. Note, however, that with these higher values for the exponents γ and ν, $\eta\approx 0.0379$ and 0.0396, respectively, which is no longer consistent with the value in (4.9), obtained by demanding K_c equality. The consistency of our results gives us additional confidence in the validity of our estimates. If we were to make the now *unreasonable* assumption that corrections to scaling vanish for the spin-1/2 Ising model, we would find $\gamma\approx 1.243$, in agreement with the analysis by Ferer and Velgakis[16] based on a 5-fit method or Guttmann[20] based on nonconfluent differential approximants; similarly, we would find $\nu\approx 0.635$. Again, with our own central estimates $\gamma=1.237$, $2\nu=1.260$, and $\theta=0.52$, we obtain from Fig. 8 the spin-1/2 Ising estimates of the correction-to-scaling amplitudes

$$a_\chi=-0.13, \qquad a_{\xi^2}=-0.22 \tag{4.11}$$

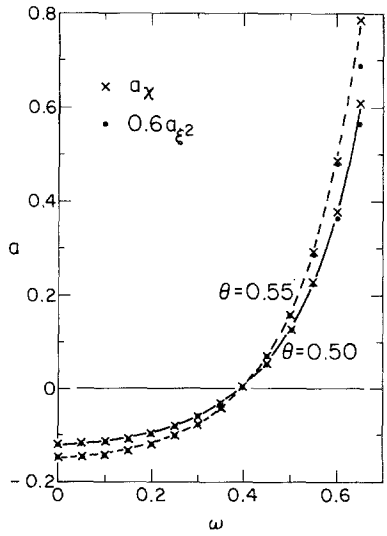

Fig. 8. Correction-to-scaling amplitudes. Estimates of a_χ (×) and $0.60a_{\xi^2}$ (●) versus ω from Fig. 7 assuming $\gamma=1.237$, $2\nu=1.260$, and $\theta=0.50$ (solid line); and from a similar plot assuming $\gamma=1.237$, $2\nu=1.260$, and $\theta=0.55$ (dashed line).

and

$$\frac{a_{\xi^2}}{a_\chi} = 1.70 \tag{4.12}$$

This same ratio estimate applies to within a few percent for all $\omega \leqslant 0.5$, as can be seen from our plot of a_χ and $0.60 a_{\xi^2}$ versus ω in Fig. 8. For $\omega \geqslant 0.5$ this ratio drops considerably and could conceivably agree with the continuum ϕ^4 model estimate[32] of 1.30 ± 0.10 in the neighborhood of the Gaussian point. As discussed in Section 1, this model dependence of the amplitude ratio is one of the indications we have for a possible absence of universality. However, given the latest continuum model estimates,[4] the value 1.30 may well be suspect.

Of course it is worth recalling from Fig. 2 that systematic trends in many of our estimates are apparent through order K^{19}. It is only because of the apparent stability of estimates based on 19-, 20-, and 21-term series and the internal consistency of results for χ and ξ^2 over a range of ω that we can have any confidence at all in our estimates. Also, the low-ω regime, and in particular the spin-1/2 Ising limit, remains notoriously difficult to analyze. Even at order K^{21}, the estimates for γ are typically bimodally distributed, as can be seen in Fig. 4. Finally, there is still a fairly large uncertainty in the value of θ and in the correction-to-scaling amplitude ratios. Thus, there is still very considerable justification for attempting to obtain even longer series.

5. EXTENSION OF SERIES

In the conclusion of the preceding section we discussed how the question of universality is not fully resolved and why there is justification for attempting to extend the available series even further. Extension by two orders in K is unlikely to lead to any significant change in these conclusions; extension by five or more orders in K is almost certainly impossible with the techniques and computer resources now available. Thus, the discussion below assumes as a reasonable goal the extension of the series to order K^{25}. At this order the array c_m used in the program segment described in Section 3 can still be packed onto a single 32-bit word, and the graph weights w can probably still be handled exactly as integers with the IBM quadruple-precision facility. Thus, large sections of the present program still can be employed without major modification.

Two features of the present program, however, must almost certainly be modified or at least receive serious attention. The first feature is apparent when we estimate the storage requirements for a naive extension

of the calculation by the program segment described in Section 3. The number of entries of 2-rooted, 1-irreducible contributions in each order n for $n = 1, 3, 5, \ldots, 19$, and 21 are 1, 2, 5, 19, 81, 353, 1619, 7704, 38,353, 204,854, and 1,055,792. Extrapolation suggests 6×10^6 and 35×10^6 entries at orders 23 and 25. At 32 bytes/entry the order-25 list would require some thirty 40-megabyte tapes for storage. However, as discussed in Section 3, each entry contains the information necessary to obtain the complete embedding constant array e_k. If we restrict ourselves *a priori* to calculations of χ and M_2 only, then the complete arrays e_k at high order are not required and a very considerable increase in packing density should be possible.

The second feature, which we believe will be the more difficult to modify significantly, is the time required for the generation of the elementary 2-rooted, 2-irreducible graphs. Our present program generates these graphs recursively by using the slightly modified Heap rules[37]: (1) Join any two existing vertices with a new bond, provided the vertices are not already linked by a bond; (2) insert a second-order vertex on any existing bond and join it to an existing vertex with a new bond, provided again that the vertices are not already linked by a bond; and (3) insert two second-order vertices on distinct existing bonds and join these by a new bond. The modifications we have introduced are for the purpose of excluding graphs with multiple bonds.

Finally, we use as the starting graph for this process the 2-rooted elementary graph shown in Fig. 9a and supplement the three Heap rules with the following: (4) Do not join the two root vertices with a new bond. We can prove that this algorithm will generate all elementary graphs by showing that for any elementary graph other than the starting graph, at least one bond can be removed which will leave the resulting graph elementary. For example, for the graph shown in Fig. 9b, any one of the four

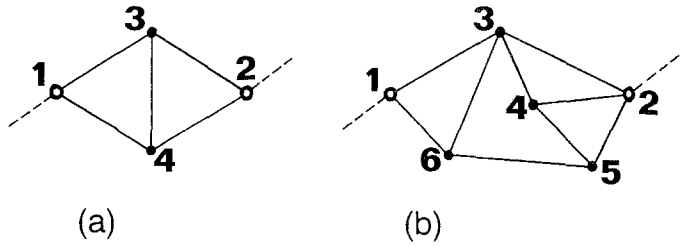

Fig. 9. Two elementary 2-rooted, 2-irreducible graphs with vertex assignments obtained from the algorithm described in the text. Each edge will eventually be replaced by a "nearest" neighbor bond or a 2-rooted, 1-irreducible segment in the bond renormalization section of the graph generating program.

bonds joining vertices 2–3, 2–4, 2–5, or 3–6 can be removed. Of course, this also shows that the graph in Fig. 9b will be generated four separate times on application of the Heap rules to lower-order graphs. Since for a general high-order graph almost all bonds can be so removed, the Heap rules are very inefficient, because of duplication. To obtain the 7×10^6 graphs estimated in Section 3 for an order-K^{25} calculation, probably in excess of 10^8 graphs must first be generated. We believe that to make an order-K^{25} calculation feasible, a more efficient algorithm to replace the Heap rules is required, and we hope some reader will be interested in this challenging theoretical design problem. Ideally, all duplication should be avoided by such a new algorithm; if this is not possible, one will still require an efficient algorithm for uniquely identifying each graph so that a tabular search can be initiated.

The algorithm we used for graph identification is probably adequate and is easily described. We begin as our step 1 by labeling the roots 1 and 2 in both possible ways. Internal vertices are labeled 3, 4,... in subsequent steps. Now in general, at the completion of step $n-1$, where $n=2, 3,...$, distinct labelings of the first n vertices will have been kept in store as possible candidates for further testing. To accomplish this testing at step n, we first scan through the labeled vertices in the first member of our candidate list in search for the largest vertex which is connected to as yet unlabeled ones. Having found this largest, say $m \leqslant n$, we proceed to assign $n+1$ in turn to every unlabeled vertex that is connected to it. For each assignment we form the integer string $mlk...$ of labeled vertices that are connected to $n+1$ with the convention $m > l > k > \cdots$. Then, of all possible labelings at this step, we keep in a temporary list those that maximize in turn l, then k,.... Since the strings to be tested will in general be of varying length, we need to imagine for this maximization that each string $mlk...$ is supplemented on the right with trailing zeros. As an example, the possible strings at $n=4$ are, in order, $4321 > 432 > 431 > 43 > 421 > 42 > 41 > 4 > 321 > 32 > 31 > 3$; the remaining $21 > 2 > 1$ never occur.

Having found the maximal string and associated (temporary) labelings for the first member in our candidate list, we proceed through the rest in a similar fashion. Either we find a smaller string, in which case the new vertex assignment is discarded, or we find a string greater than or equal to the previous maximal. If greater, all preceding temporary lists are discarded, but in both this and the equals case the new labeling is incorporated as part of our (temporary) list. On testing completion this list becomes the possible candidate list for step $n+1$. Note that the discard process makes the algorithm relatively efficient; each list length is the symmetry number of the partially labeled graph and this typically is quite small.

When the labeling is finally complete, we use as the unique graph

identifier the composite integer string formed from the individual strings generated at $n = 2, 3, \ldots$ and listed from left to right with a single 0 between string segments. As an example, the algorithm generates the unique strings 210321 and 210320420531 for the graphs in Fig. 9. Furthermore, it shows that the corresponding labeling in Fig. 9b is unique, whereas the labeling in Fig. 9a is only one of four symmetry equivalent ones—essential information for the subsequent bond renormalization segment of our program.

Given the integer strings generated as described above, graph comparisons are easily made by an individual integer-by-integer comparison or, equivalently, by number comparison where each graph is the single number that is the string in a system with an appropriate radix. For a list of *all* elementary graphs of $\leqslant 25$ bonds, a radix $\geqslant 17$ is necessary, but in fact, such a complete list is not required and radix 16 is both adequate and convenient for packing all strings on at most five 32-bit words.

The elementary list reduction comes from the fact that for a calculation of zero-field χ and M_2 on the bcc lattice family, every elementary graph must, after bond renormalization, contain only even-order internal vertices and even loops so that it can be embedded on a linear chain or a pair of nearest-neighbor sites. For example, the even-order vertex requirement can be achieved by doubling bond 3–4 in Fig. 9a and bonds 1–6 and 4–5 in Fig. 9b. The even-loop requirement can be achieved by the insertion of a second-order vertex on bond 3–4 in Fig. 9a and on bonds 1–3 and 2–4 in Fig. 9b. Other doublings and insertions may also work, but in any case the graphs in Fig. 9 cannot contribute at orders lower than the "true" orders defined by the addition of these minimal doublings and insertions to the direct bond counts, i.e., $5 + 1 + 1 = 7$ and $9 + 2 + 2 = 13$. These "true" orders are the ones used for the graph counts given in Section 3, but the Heap rules were not completely successfully supplemented to avoid redundancy by generating graphs of too high "true" order.

In summary, we believe the derivation of an efficient algorithm to replace the Heap rules for graph generation represents a challenging theoretical problem whose solution would be of great practical use in making possible the extension of the series now available.

ACKNOWLEDGMENTS

The authors thank M. E. Fisher and G. A. Baker for discussions and suggestions. This work was supported in part by NSERC (B.G.N.) and by NSF grant DMR 82-07357 (J.J.R.).

REFERENCES

1. G. A. Baker, Jr., and J. M. Kincaid, *J. Stat. Phys.* **24**:469 (1981).
2. M. E. Fisher, *Rep. Prog. Phys.* **30**:615 (1967).

3. M. A. Moore, D. Jasnow, and M. Wortis, *Phys. Rev. Lett.* **22**:940 (1969).
4. J. C. Le Guillou and J. Zinn-Justin, *Phys. Rev.* **21**:3976 (1980); *J. Phys. Lett.* (Paris) **46**: L-137 (1985); *J. Phys.* (Paris) **48**:19 (1987).
5. B. G. Nickel and B. Sharpe, *J. Phys. A: Math. Gen.* **12**:1819 (1979).
6. D. S. Gaunt and M. F. Sykes, *J. Phys. A: Math. Gen.* **12**:L25 (1979).
7. J. Zinn-Justin, *J. Phys.* (Paris) **40**:969 (1979).
8. D. S. Gaunt, in *Phase Transitions: Cargèse 1980*, M. Levy, J. C. Le Guillou, and J. Zinn-Justin, eds. (Plenum Press, New York, 1982), p. 217.
9. B. G. Nickel, in *Phase Transitions: Cargèse 1980*, M. Levy, J. C. Le Guillou, and J. Zinn-Justin, eds. (Plenum Press, New York, 1982), p. 291.
10. J. Zinn-Justin, *J. Phys.* (Paris) **42**:783 (1981).
11. P. Moussa, *J. Stat. Phys.* **27**:711 (1982).
12. R. Z. Roskies, *Phys. Rev. B* **24**:5305 (1981).
13. J.-H. Chen, M. E. Fisher, and B. G. Nickel, *Phys. Rev. Lett.* **48**:630 (1982).
14. B. Nickel and M. Dixon, *Phys. Rev. B* **26**:3965 (1982).
15. J. Adler, M. Moshe, and V. Privman, *Phys. Rev. B* **26**:3958 (1982).
16. M. Ferer and M. Velgakis, *Phys. Rev. B* **27**:2839 (1983).
17. J. L. Gammel and D. C. Power, *J. Phys. A: Math. Gen.* **16**:L359 (1983); J. L. Gammel, J. Nuttal, and D. C. Power, St. Louis University Preprint (1983).
18. M. J. George and J. J. Rehr, *Phys. Rev. Lett.* **53**:2063 (1984).
19. M. E. Fisher and J.-H. Chen, *J. Phys.* (Paris) **46**:1645 (1985).
20. A. J. Guttmann, *J. Phys. A: Math. Gen.* **20**:1855 (1987).
21. A. J. Liu and M. E. Fisher, *Physica A* **156**:35 (1989).
22. B. Nickel, *Physica* (Utrecht) **106A**:48 (1981).
23. J. J. Rehr and B. Nickel, *J. Stat. Phys.* **24**:710 (1981).
24. J. J. Rehr and B. G. Nickel, *Bull. Am. Phys. Soc.* **26**:242 (1981).
25. M. Blume, *Phys. Rev.* **141**:517 (1966); H. W. Capel, *Physica* **32**:966 (1966).
26. J. R. Klauder, *Ann. Phys.* (N.Y.) **117**:19 (1979).
27. G. A. Baker, Jr., and A. R. Bishop, *J. Phys. A: Math. Gen.* **15**:L201 (1982).
28. J. J. Rehr, G. S. Joyce, and A. J. Guttmann, *J. Phys. A: Math. Gen.* **13**:1587 (1980).
29. M. E. Fisher and R. M. Kerr, *Phys. Rev. Lett.* **39**:667 (1977); M. E. Fisher and H. Au-Yang, *J. Phys. A: Math. Gen.* **12**:1677 (1979).
30. F. J. Wegner, *Phys. Rev. B* **5**:4529 (1972).
31. F. S. Acton, *Numerical Methods That Work* (Harper and Row, New York, 1970), p. 552.
32. C. Bagnuls and C. Bervillier, *Phys. Rev. B* **24**:1226 (1981).
33. M. Wortis, in *Phase Transitions and Critical Phenomena*, Vol. 3, C. Domb and M. S. Green, eds. (Academic Press, London, 1974), p. 113.
34. D. E. Knuth, *The Art of Computer Programming*, Vol. 3 (Addison-Wesley, Reading, Massachusetts, 1973).
35. M. A. Moore, D. M. Saul, and M. Wortis, *J. Phys. C: Solid State* **7**:162 (1974).
36. G. S. Joyce, in *Phase Transitions and Critical Phenomena*, Vol. 2, C. Domb and M. S. Green, eds. (Academic Press, London, 1972), p. 375.
37. B. R. Heap, *J. Math. Phys.* **7**:1582 (1966).

APPENDIX

Spin-S, Blume–Capel, Klauder, and double-Gaussian series coefficients (Tables I–IV) and representative differential approximants (Table V).

Table I

- - - SPIN - S MODEL - - -
SUSCEPTIBILITY AND SECOND MOMENT . . . DIMENSION = 2

	S = 1/2		S = 1	
0	1.0000000000000000000000Q+00		1.0000000000000000000000Q+00	
1	4.0000000000000000000000Q+00	4.0000000000000000000000Q+00	4.0000000000000000000000Q+00	4.0000000000000000000000Q+00
2	1.2000000000000000000000Q+01	3.2000000000000000000000Q+01	1.3000000000000000000000Q+01	3.2000000000000000000000Q+01
3	3.4666666666666666666667Q+01	1.6266666666666666666667Q+02	4.1500000000000000000000Q+01	1.6950000000000000000000Q+02
4	9.2000000000000000000000Q+01	6.8266666666666666666667Q+02	1.2306250000000000000000Q+02	7.6000000000000000000000Q+02
5	2.4053333333333333333333Q+02	2.5445333333333333333333Q+03	3.6116875000000000000000Q+02	3.0651687500000000000000Q+03
6	6.1120000000000000000000Q+02	8.7694222222222222222222Q+03	1.0259171875000000000000Q+03	1.1537700000000000000000Q+04
7	1.5381841269841269841270Q+03	2.8554717460317460317460Q+04	2.8931965401785714285714Q+03	4.1255396540178571428571Q+04
8	3.8096380952380952380952Q+03	8.9094501587301587301587Q+04	8.0196601771763392857140Q+03	1.4193716964285714285710Q+05
9	9.3646589065255731922400Q+03	2.6877528324514991181660Q+05	2.2102271487862723214290Q+04	4.7348903934500558035710Q+05
10	2.2820767830687830687830Q+04	7.8918684895943562610230Q+05	6.0294806390032087053570Q+04	1.5407662743638392857140Q+06
11	5.5317567086740420073750Q+04	2.2659737905788039121370Q+06	1.6374218968909325537740Q+05	4.9108568172114146839490Q+06
12	1.3326715320827320827320Q+05	6.3855138811950189727970Q+06	4.4171672024140692376470Q+05	1.5382142548845246550320Q+07
13	3.1986228507558285336060Q+05	1.7709494299441463885910Q+07	1.1874205448825629250510Q+06	4.7466266768897122584140Q+07
14	7.6429636402229164133930Q+05	4.8444751835308442292570Q+07	3.1770075304978286976720Q+06	1.4459352939922591977990Q+08
15	1.8209987787468435934040Q+06	1.3094385993194469571190Q+08	8.4769076722760831502970Q+06	4.3551393000973700173090Q+08
16	4.3242148021424877297890Q+06	3.5023136244918069663040Q+08	2.2538751806345544262470Q+07	1.2987660932172101170990Q+09
17	1.0244937682000539880400Q+07	9.2805603779715601227400Q+08	5.9795259897014746908120Q+07	3.8389375228840613244890Q+09
18	2.4209158084666510167910Q+07	2.4388324973056151458470Q+09	1.5820505554189323432010Q+08	1.1257743131651793220580Q+10
19	5.7101307501135767439230Q+07	6.3613012421600429641180Q+09	4.1782541749296854011100Q+08	3.2778728682531563394550Q+10
20	1.3440093637601427882470Q+08	1.6480959395838424212570Q+10	1.1010950799735048264260Q+09	9.4826624048492331099170Q+10
21	3.1586042332335933275030Q+08	4.2438700480233964556550Q+10	2.8974000514613839727690Q+09	2.7272063228603683395090Q+11

	S = 2		S = INF	
0	1.0000000000000000000000Q+00		1.0000000000000000000000Q+00	
1	4.0000000000000000000000Q+00	4.0000000000000000000000Q+00	4.0000000000000000000000Q+00	4.0000000000000000000000Q+00
2	1.3400000000000000000000Q+01	3.2000000000000000000000Q+01	1.3600000000000000000000Q+01	3.2000000000000000000000Q+01
3	4.4326666666666666666667Q+01	1.7232666666666666666670Q+02	4.5760000000000000000000Q+01	1.7376000000000000000000Q+02
4	1.3739416666666666666667Q+02	7.9242666666666666666670Q+02	1.4498285714285714285710Q+02	8.0896000000000000000000Q+02
5	4.2252208333333333333333Q+02	3.2954820833333333333330Q+03	4.5628734693877551020410Q+02	3.4156473469387755102040Q+03
6	1.2595164513888888888889Q+03	1.2845855555555555555560Q+04	1.3940819591836734693880Q+03	1.3547363265306122448980Q+04
7	3.7326014124007936507940Q+03	4.7699336879067460317460Q+04	4.2374640326530612244900Q+03	5.1262611853061224489800Q+04
8	1.0871771562729414682540Q+04	1.7080997228730158730160Q+05	1.2664136893506493506490Q+04	1.8730554932244897959180Q+05
9	3.1514134665618455136680Q+04	5.9404604498202057153880Q+05	3.7686628774363299038620Q+04	6.6529128013762860516110Q+05
10	9.0387104969068097580470Q+04	2.0180576215033476631390Q+06	1.1096910518031074676710Q+05	2.3100832486403084114400Q+06
11	2.5823001074726745897090Q+05	6.7218490368337727473310Q+06	3.2559152340068161127950Q+05	7.8696057728555533210700Q+06
12	7.3259255907675261101030Q+05	2.2022353491562670951410Q+07	9.4855204977466595008690Q+05	2.6383427602712100740300Q+07
13	2.0717786787281612363100Q+06	7.1129051433667261585190Q+07	2.7553507924863735733370Q+06	8.7237605111241834765040Q+07
14	5.8301286887101568986950Q+06	2.2692541901345798284140Q+08	7.9635160330946720758840Q+06	2.8503113294302931143690Q+08
15	1.6364359308935774513400Q+07	7.1617285690951474037680Q+08	2.2960618021924182132260Q+07	9.2153853015489116884480Q+08
16	4.5764631244828108347810Q+07	2.2387686583129175875510Q+09	6.5953539916558755061150Q+07	2.9519541341943293195610Q+09
17	1.2771737946673920269930Q+08	6.9390938744604142167280Q+09	1.8906977681252050984560Q+08	9.3779378126966535407210Q+09
18	3.5542329153482715430200Q+08	2.1346018123133920492670Q+10	5.4045059911281535678540Q+08	2.9572292424962147551830Q+10
19	9.8738901463984917714440Q+08	6.5205727036755596756730Q+10	1.5422743051916806754730Q+09	9.2629758246422946421790Q+10
20	2.7368990624549760799200Q+09	1.9796078615015760482290Q+11	4.3911310098723589245780Q+09	2.8838926344823650644360Q+11
21	7.5752780253104561660810Q+09	5.9759505822852986559820Q+11	1.2484647798122697661780Q+10	8.9289522073303358652520Q+11

Table I. *(Continued)*

- - - SPIN - S MODEL - - -
SUSCEPTIBILITY AND SECOND MOMENT . . . DIMENSION = 3

	S = 1/2		S = 1	
0	1.000000000000000000000000Q+00		1.000000000000000000000000Q+00	
1	8.000000000000000000000000Q+00	8.000000000000000000000000Q+00	8.000000000000000000000000Q+00	8.000000000000000000000000Q+00
2	5.600000000000000000000000Q+01	1.280000000000000000000000Q+02	5.800000000000000000000000Q+01	1.280000000000000000000000Q+02
3	3.893333333333333333333333Q+02	1.413333333333333333333333Q+03	4.190000000000000000000000Q+02	1.443000000000000000000000Q+03
4	2.610666666666666666666667Q+03	1.348266666666666666666667Q+04	2.939125000000000000000000Q+03	1.417600000000000000000000Q+04
5	1.747306666666666666666667Q+04	1.178250666666666666666667Q+05	2.059133750000000000000000Q+04	1.282393375000000000000000Q+05
6	1.152504888888888888888889Q+05	9.747256888888888888888889Q+05	1.423789093750000000000000Q+05	1.101985800000000000000000Q+06
7	7.595457015873015873015873Q+05	7.751144634920634920634920Q+06	9.839016680803571428571430Q+05	9.122911268080357142857140Q+06
8	4.966694577777777777777778Q+06	5.989593640634920634920630Q+07	6.749890203278459821428570Q+06	7.351293925357142857142860Q+07
9	3.245860521199294532627870Q+07	4.525398777622574955908290Q+08	4.628832750000697544642860Q+07	5.798716606428641183035710Q+08
10	2.111009732650440917107580Q+08	3.359417571573615520282190Q+09	3.159764853630786132812500Q+08	4.498392313133727678571430Q+09
11	1.372341126969094115760780Q+09	2.457880965684168670835340Q+10	2.156297083295681199903610Q+09	3.441747552464085977133220Q+10
12	8.892253404658017209128320Q+09	1.776964585165889070600180Q+11	1.466894073423915768511880Q+10	2.603627871224436259638800Q+11
13	5.759904658730236216458440Q+10	1.271702444659990128719020Q+12	9.976673547851515075706460Q+10	1.950600378053968985984340Q+12
14	3.722158877490608999231220Q+11	9.023080239545997126025060Q+12	6.769910936120329710742300Q+11	1.449418056240361100795250Q+13
15	2.404682094485187424344420Q+12	6.354288372882067088755260Q+13	4.592992520006030527807210Q+12	1.069304613834047298339160Q+14
16	1.550776349705173888672490Q+13	4.445853320509161515977390Q+14	3.110702880340500511393260Q+13	7.839863887418436637988320Q+14
17	9.998735146106036599647410Q+13	3.092713794567894824964340Q+15	2.106448563794377154440180Q+14	5.716282054493223273594340Q+15
18	6.437833862537838781754880Q+14	2.140502411181645393890980Q+16	1.424478580827764706305290Q+15	4.147642231609886401676490Q+16
19	4.144333549231027851402080Q+15	1.474712492834961376203290Q+17	9.631661389329921610232710Q+15	2.996271993138698408989740Q+17
20	2.664945141465304959880820Q+16	1.011869402839301296448260Q+18	6.505408399069703078493940Q+16	2.156037057558294300709840Q+18
21	1.713382087746695175104720Q+17	6.917197356974289187835550Q+18	4.393357283073530449022580Q+17	1.545892417474300336298820Q+19

	S = 2		S = INF	
0	1.000000000000000000000000Q+00		1.000000000000000000000000Q+00	
1	8.000000000000000000000000Q+00	8.000000000000000000000000Q+00	8.000000000000000000000000Q+00	8.000000000000000000000000Q+00
2	5.880000000000000000000000Q+01	1.280000000000000000000000Q+02	5.920000000000000000000000Q+01	1.280000000000000000000000Q+02
3	4.310533333333333333333333Q+02	1.455053333333333333333333Q+03	4.371200000000000000000000Q+02	1.461120000000000000000000Q+03
4	3.078935000000000000000000Q+03	1.445930666666666666666667Q+04	3.150674285714285714285710Q+03	1.460224000000000000000000Q+04
5	2.197092416666666666666667Q+04	1.326090041666666666666667Q+05	2.269031183673469387755100Q+04	1.348387918367346938775510Q+05
6	1.549111061250000000000000Q+05	1.156979430222222222222222Q+06	1.615707324081632653061220Q+05	1.185392890775510204081630Q+06
7	1.091706408891468253968250Q+06	9.735032441958134920634920Q+06	1.149995743608163265306120Q+06	1.005571200731428571428570Q+07
8	7.641474867794010416666670Q+06	7.979282533894920634920630Q+07	8.132334904828200371057510Q+06	8.313028544702040816326500Q+07
9	5.346963242452247368276010Q+07	6.405957676400314683917550Q+08	5.749191635646672288750210Q+07	6.733487591251850902344410Q+08
10	3.752219443628534711888820Q+08	5.060190850471477973985890Q+09	4.047494937224021971349620Q+08	5.367791534858265659831820Q+09
11	2.594711398211273553271120Q+09	3.943721388800275777549330Q+10	2.848844397517756910714560Q+09	4.222770750975139734741970Q+10
12	1.801868790755766305888600Q+10	3.039890311185978060639310Q+11	1.999361888285415566965800Q+10	3.286144265606852108501150Q+11
13	1.251040085632647097011770Q+11	2.321171249093480500360550Q+12	1.402930659872296232016770Q+11	2.533581262469373115423200Q+12
14	8.666964729329296336817435Q+11	1.758270173415415174138890Q+13	9.823276447474208673428010Q+11	1.938050504156493676178230Q+13
15	6.003326420694838787275620Q+12	1.322584415792078346280700Q+14	6.877209124815880661707300Q+12	1.472309261434454917701870Q+14
16	4.151372129131007614425150Q+13	9.888451107369174537264520Q+14	4.806860207549086653081940Q+13	1.111831643000663402859980Q+15
17	2.870329847188902283577450Q+14	7.353401224113057897937690Q+15	3.359360311837451711518990Q+14	8.351555217213971165965000Q+15
18	1.981991586038871684828600Q+15	5.442292000165040301206980Q+16	2.344739780949245188197180Q+15	6.243943066671210550513700Q+16
19	1.368424846927330353820970Q+16	4.010619285444669530906120Q+17	1.636388268217570962179180Q+16	4.648493086789075222090830Q+17
20	9.438010339071734948375520Q+16	2.944256749539989858254350Q+18	1.140848501725564868228930Q+17	3.447650988335769487322720Q+18
21	6.508725641537647365480200Q+17	2.153884103440522500804300Q+19	7.952971132629686635313820Q+17	2.548221155117613724844680Q+19

Table II

--- BLUME - CAPEL MODEL ---

SUSCEPTIBILITY ... DIMENSION = 2

1			7490801/32	98166157/64
			26066973/16	781452353/64
			605732763/64	11255253387/128
4			219188835/4	33488222931/64
			1925261193/8	216605005223/64
10	10651/4	559987/16	5126209227/4	570356755971/32
4	43985/4	1633671/8	75995388557/16	4276354557853/48
	163211/4	3947691/4	16195021131	3989983050753/8
22	107106	17629131/4	1231520406093/20	657843602816 19/40
24	329634	74013625/4	240596608203/2	588628442798 97/8
4	869199/2	212011305/4	1003629813297/8	100308028052911/4
	680041/3	2412862115/12	70490914560	97559553870681/2
43	46110	410907970	309308139619/14	667450059148823 9/120
81	1532	404757006	2504482379	151023064659679/40
50	4	202726455	569602065/4	113860791934589/8
4		43566090	92520	3013411443679
	5275	3931650	4	961500149484/5
88	22002	122860/7		30675328677/5
196	196395/2	4	27925957/64	786430
309	285642		207547895/64	4
72	3520379/4	2147513/32	1259440045/64	
4	2170848	1585669/4	1908956155/16	45502945/16
	12240635/6	36090085/16	57763102283/96	95829355/4
184	2327248/3	9548506	46764445089/16	11291067127/64
429	642606/5	572468305/12	355515973763/24	9395226769/8
1066	2232	161431041	556065647983/12	337450098763/48
810	4	1076961565/2	160167479857 7/8	37251057624 9/8
460/3		1806192488	468691882245 5/8	4120394862748 1/192
4	19871/2	28498605891/10	223786455079 55/24	3893122086920/3
	188221/4	2232780648	83716613895 0	4647628748383 5/80
761/2	209692	934648055	873135723459 2/21	8253024408209 9/4
968	794713	157226592	45606835309 1/4	4506858003746 351/48
2765	2660691 7/12	438492622/35	66419455505/6	5323930819970 73/2
4672	30331653/4	131064/5	497097750	6084973830231 0837/140
2146	150740321/12	4	1966060/9	2125637345428 11/5
216	9377997		4	1010388122412 67/4
4	15187948/5	8104693/64		8182991178516 0
	401391	50791079/64	26377013/32	154753407617 16
2893/4	15350/3	303176237/64	50149469/8	752702568948
9447/4	4	728751513/32	6757404 59/16	1525240002 15/7
25257/4		3429341747/32	977978991/4	8388600/7
33657/2	147731/8	3927311127/8	96737593005/64	4
17232	202609/2	235612644 53/16	54288113685/8	
11889/2	3502471/8	6001690399	3725952204785/96	
475	1999953	593793807303/40	471164145530/3	
4	12652921/2	151148622717/8	219447811404 5/4	
	20203668	102132369459/8	2301482749320	
2699/2	177713333/3	18552416157/4	219269738284 25/4	
5399	216417880/3	23529911302/35	72133438999 95	
62713/4	42578200	851121261/20	132723128793973/24	
43960	10612700	122875/2	7007991950932/3	
282085/3	1200815	4	6767832713075/12	
60670	7560		127133754160/3	
93755/6	4		5168442538/3	
680			331128	
4			4	

Table II. *(Continued)*

	--- BLUME - CAPEL MODEL ---			
	SECOND MOMENT ... DIMENSION = 2			
4			1368871009/32	1523305685/4
			3976013565/16	5339390595/2
32	178660	17754287/4	79079099931/64	31848321405/2
0	530728	40816689/2	21492918339/4	1700152217317/2
	1329130	161367009/2	168332797113/8	1673999758595/4
150	2369760	266383686	287216656011/4	7526801737959/4
24	2706550	753628390	3359725676173/16	1828174918660517/24
4	1617756	1705206360	486336204939	26982897733351
	1485628/3	8110405930/3	15711599782989/20	81871893032853
544	176032/3	2660274320	1664255871243/2	1928689113706321
256	8192/5	1572269340	4529168436273/8	3235723133218420
64	0	514676040	228573028224	3715149219520201
0		78156120	736404073187/14	428190041890245 8/15
	409877	4410720	4530041163	7014374353148265
1688	1386114	131072/7	630373905/4	4028684405692 1
1476	7963707/2	0	92520	626246204987 2
693	8732010		4	1548340669232/5
72	55867067/4	305553801/32	178666959/2	31502070432/5
4	12820608	190991461/4	554673073	4194304/5
	40098907/6	3283914157/16	23555452529/8	0
4740	1659120	751338794	13779547979	12454029621/16
6232	180054	28792285889/12	1409434201033/24	5770518816
5128	2232	6402885657	888891089931/4	23219383003 99/64
1376	4	26476280869/2	293081277507 9/4	1642911506721/8
512/3		18087264680	60903674305 18/3	5175608505460 7/48
0	921480	1564740854 43/10	42432972631 72	4167747120286 5/8
	3493252	8058345768	17266031846045/3	1472174342105299/64
24953/2	11309260	2382897751	3478978104120	2706960297355 04/3
21768	29092520	295440480	880405748454 5/7	2473505129933295 1/80
27373	178694708/3	103004022/7	74482488626 6/3	3525219967364707/4
14400	79731684	131064/5	54745818670/3	9035871635355343 9/48
3810	63176826	4	1559833760/3	5674903204686177/2
216	82112048/3		2097152/9	4135944792086020 21/140
4	29375344/5	40622615/2	0	1027864329647277 1/5
	475936	2195564 09/2		3696369718094163/4
31352	16384/3	2035951513/4	5924274569/32	2345055484677 84
67656	0	2041237599	9785528565/8	3363837566456 4
115116		7260905045	1103887240 15/16	1300891844340
103728	162972 11/8	22098159162	138256735623/4	158103255255/7
47376	17093537/2	55740428090	10164731858205/64	8388600/7
8352	2461081 19/8	101788286960	5270665661685/8	4
512	90386817	6129317123 76/5	2321765932 99385/96	
0	4437640 73/2	92965717368	2298680944 6810/3	
	4012360 68	42584408916	7921853762 3041/4	
1519 47/2	1380310757/3	10759263984	3697379128 6440	
194679	309402184	40144289776/35	1891860602 36905/4	
1650937/4	119619416	229014304/5	4014105040 5675	
552504	21033180	65536	5288555725 52629/24	
1239845/3	1527855	0	704663296 5484	
146430	7560		1530699761 5315/12	
48745/2	4		7461529320 0	
680			1831563790	
4			331128	
			4	

Table II. *(Continued)*

--- BLUME - CAPEL MODEL ---

SUSCEPTIBILITY ... DIMENSION = 3

1		
8		
52	179333501/2	848834064671/8
8	315337853/2	2707094986 76
	402477745/2	1032573675309/2
332	191154122	815463459528
112	123748280	1076018103370
8	44904249	1136158121010
	23831812/3	264625943934 5/3
2014	1629508/3	1355215258780/3
1114	35752/5	140550166560
236	8	24064561410
8		1887940080
	527680859	46677780
12200	1032347656	573352/7
9304	1482986070	8
3642	1653359784	
336	2734012901/2	9926065952507/16
8	719303136	3411273156879/2
	614753033/3	281352179693 71/8
72820	83342368/3	6079543970266
70358	7502556/5	537076521174 49/6
41032	10416	10928695598008
9764	8	10404750630245
2152/3		7022054413056
8	6189112937/2	153372945208 29/5
	6668756859	808593314016
434759	42535992535/4	117204148858
505696	27083295469/2	7358391552
390814	40549415617/3	5195932892/35
158272	19097051029/2	611632/5
24836	24976408141/6	8
1008	2999361514/3	
8	577815484/5	1158561821639 51/32
	4744294	3415053 10054853/32
5147651/2	71636/3	7567196602680 85/32
7011181/2	8	709710772631825/16
6635847/2		1150782998408317/16
1969419	72571696703/4	7936010494131 27/8
591546	42689348702	892051955251855/8
70173	74773670896	94924832884436
2218	106774945636	1125994390151541/20
8	124108777947	870191910805 71/4
	109689355482	204249954622 89/4
15231653	197042233948/3	1290917220759/2
23753006	70466166512/3	121238230095 1/35
52934779/2	4643970632	5071570697/10
20558744	425187560	286709
28704770/3	14133070	8
2038900	35280	
543395/3	8	
9520/3		
8		

337999003449551/16	83438039503521 65/2
5316203712485 09/8	1248308428890952 21/8
5038005712078005/32	2822477231695466439/64
318219219370902	3457376634418557759/32
562596476154111	7586751385283454571/32
862296748168428	7480273919979931017/16
44484613530285 79/4	1967910637945036011 5/24
1140771625305572	1500489811398552565/12
8626109963903631/10	1596699096184674041 7/10
447284913349581	16206673443649049 9
6030214029911 31/4	9905269728132763565/8
30607971878124	2721867622976178033/4
232514449200 43/7	3862965025006902922/15
142417371554	3788772137739228521/60
3391198185/2	3620713422233366 9/4
431760	639119567487226
8	781440652462 12/5
	367189984098/5
3938596883481155/32	18350036/5
1317048734859993 1/32	8
3321539076797315 3/32	
8989912603180325/4	3883385995499273 33/16
2062583628373665 49/48	7646943209577525 45/8
7228011837803777	9108937168177295323/32
1256943933629418 37/12	2949969591832283507/4
12547974973633538	4129886005202835565 3/24
467461375994595 61/4	1454613599353935 0667/4
316477345042273 25/4	6635737210236016437 05/96
442697915847830 95/12	1161719560091802 0876
7121490377941045	6708622217328556468 03/40
4295070878851400/21	1992015359021490 0611
1159356808038 23/6	1109252102902962 22271/6
21137781772 30/3	1278680802686 3186338
178202275 40/3	4440067847733477586 99/70
9174952/9	1080132903563937 8599/5
8	9480392137512 48531/2
	5957552812947 8064
2867967100303733/4	3636443008060896
2539584381229660	69818071889016
5433333693789337 7/8	1825417595870/7
3135165036332 13359/2	5592400
1030367578173376835/32	8
2354892354992 10495/4	
4531713925406209595/48	
3863986592550 35210/3	
1423012907147 14798	
1196115498858 05260	
72227167172517000	
2992445131732 0140	
9678573871560 6187/12	
3856258851241664/3	
629166985392785/6	
9095937931360/3	
61736670548/3	
1545264	
8	

Table II. *(Continued)*

--- BLUME - CAPEL MODEL ---				
SECOND MOMENT ... DIMENSION = 3				
8			13650158907887311/16	208189004403572123
			17918801289824925/8	133761231863614726 5/2
			139484352615527637/32	32098932113620167 45/2
			7064497955305590	32839001443621531 56
			9720762020932767	11795262647352872443/2
128	1812419584	66571845327 85/2	11188304967714156	18575282200353387627/2
0	2305499752	6794978329491	41794208549573411/4	15176127537534572 4389/12
	2033082304	10128886987401	7587422744894436	14541162411979787486
1356	1229156256	12034540346328	8191156099518243/2	68458589267995258542/5
112	483890196	11406722341240	1570306992626637	10198097706221236476
8	108868344	8253411465360	1623382357067547/4	58054055836666842 40
	38979400/3	12915673543960/3	64564349710572	24360440283135761 28
12160	1760320/3	1514128025760	5557857384317	21612574899946828 60/3
2560	32768/5	337254452424	183459412386	70032605082789778 8/5
256	0	42274934160	3634285545/2	160953522656772 30
0		2517330000	431760	901268637561376
	12072556423	44107200	8	17857827824032
98728	17659802760	524288/7		63004140864
35928	18257446782	0	5356037371029579	16777216/5
6714	13685522472		302171313569666127/2	0
336	14354738981/2	340548378083787/16	126759733320392203/4	
8	2381942112	95167254190063/2	5587733588680342	20642581243081715901/16
	1408333129/3	6253048555943 71/8	10171838378864180 15/12	35181408019481084397/8
752856	45944160	1042048631296 90	21924903903123954 9/2	35893331737846419623 5/32
401968	9563868/5	6822499547167 13/6	23604458482548061 1/2	98103370401167045531/4
121840	10416	98375451411960	30628402646731650 4/3	11383577162293012416 53/24
13760	8	64355170298109	68122548940416376	32516545330677570 0915/4
2048/3		300462272724 48	33614283424005140	39097345694293605764 83/32
0	79388688432	47548563161469/5	352600651575875 60/3	47390078302451531 7220/3
	13137195816	1889912282592	2743003528515840	68476161962555565443 31/40
5493959	155829388960	212293385594	27371745329076 46/7	15080977238295898 6187
3913312	139617303008	10171664640	863253460093 64/3	62786487105244178 5939/6
1711262	27757536 3320/3	5808152796/35	2510228440900/3	55428990789636708354
360000	41925993432	611632/5	15598337600/3	30298400434747227 22583/14
38148	12078336460	8	8388608/9	29643330305186983143/5
1008	5992734944/3		0	21219935746093767 87/2
8	167836448	135163561548199		10907199438680107 2
	4759360	32849361620103 7	33464450075837594	5434356165210720
38835920	65536/3	11789387154916 07/2	100947496887759136	80852066866296
34797168	0	870867136353894	18159883646762043 13/8	187004843619 07/7
20241000		10746862906208 94	86487629726665 3383/2	5592400
6672864	20656952441 51/4	10833527890084 56	22928881709240203155/32	8
1173600	954211673774	858528851606960	41116871793806599 35/4	
83520	1277160911564	508545018315104	60166393973973873635/48	
2048	1331187088548	214201647277584	37859565156777726 50/3	
0	1070993998515	60672641619024	10123169124149468 36	
	626682392154	10746827253720	62286588792540750 0	
267866325	749697731356/3	1032238914912	28341091138750194 0	
290061102	189294496496/3	302852013344/7	91244313628343820	
423883003/2	9298861768	458028608	23474144520767946 7/12	
98123672	638363880	262144	75139774583444 48/3	
81212290/3	16749390	0	98826186088430 5/6	
3810420	35280		3682727276600	
251105	8		21448887068	
9520/3			1545264	
8			8	

Table III

--- KLAUDER MODEL ---

SUSCEPTIBILITY ... DIMENSION = 2

1			46620662575398912000	25510826561258284646400000
			-290832373536227523000	-19542354718348970695687500
2			847107357402349212750	708658923732041471203192500
			-15208879236503975370000	-16109435274629005883250855O
			1873605108497706472248	256428425812095191844746010
8	3715891200	1428329123020800	-167003719759346702568O	-30259282764218689984843024 2
-2	-11588516100	-6947833630537800	11077489284960669526O4	2735164512390981372434248480
	15697622430	15462636059613645	-55428563759197635132O	-19307879792868574674573727 6
48	-11892097614	-2067246191409048 9	2099046334200912204 36	10758185926580278219309524 0
-24	5434843048	183639635765828 82	-59800206931600635776	-47511356787127289244391016
2	-1514155556	-113417163774389 14	126080561363303784 24	16604416970731022268518408
	248116064	495916380140558 3	-19080429425957539 20	-45579190848693017537801 52
384	-21598072	-153511022602471 7	1965685871472410 24	9685683244694441871315 04
-318	771456	330693777947296	-12532944323132928	-15557917774675022306684 80
76	-5760	-476487435714 36	40493447587584 0	18189367971408945375744
-4		4247211891792	-3382622208000	-14560583337843694214 40
	81749606400	-199048783536	3251404800	7168639889810325196 8
3840	-289344409200	3172815360		-17233912188257126 40
-4440	452110350375	-7257600	167834385271436O832000	7342962846105600
1718	-404293119846		-11260925079619375660500	-2633637888000
-224	225220391219	428498736906240 00	3546678128496299884 3950	
8	-80068102576	-227740501880892000	-69313026882968970795270	10714547155728479551 4880000
	17950890408	557986870793966512.5	937009126687086198680 76	-87216547633141119656 4630000
46080	-2415998200	-829248050414243295	-92551363515658097080776	33720879845446831627 33944375
-70380	173499776	828908926880955691.5	68833018580422671182628	-82060047439498535754 09672900
40158	-4963200	-584971695998572974	-39171000529076374969056	14049700999197882234 919317900
-9918	28800	29804254038773729 4.5	171673994182908674075 04	-17931468972939822766616895108
960		-110298120392103637	-57860044719011000099 64	17644337478016366060139180715
-24	1961990553600	2942799385343744 8.5	14853685919454174718 08	-13661881170306548373133427184
	-7802021096100	-55334909774261 92	-28485733565120972853 6	84247683910287095682280182 20
645120	13903173908730	701121591342872	3946744446209659328	-41622430228267834283190659 04
-1224720	-14477912874558	-55010892645504	-37348417690119388 80	16488695726438544212784129 12
916491	9663069095550	224269415870 4	2184240740766721024	-52163047574840256286065456 8
-327702	-4278032936622	-28689292800	-6389688112473600	13053264279767792811282219 6
55145	1259741047224	50803200	435588378624 00	-25420375305865272952799280
-3840	-240823400136		-29262643200	37554698492405798533772 96
72	28110117840	13711959580999680 00		-40460599822731114382297 60
	-1751115360	-79207946997446767 50	63777066403145711616000	29850834873786681894912
10321920	41633280	21244383335539872900	-45797161905351329873 4000	-13515875032044533299 20
-23721390	-172800	-34879288598505870660	15503392276342933946082 75	29630170235175321600
22489236		38960385993267912396	-32735535737758143601592 70	-95851418148864000
-11017588	51011754393600	-31163806868759749140	4811192307588574352676897	26336378880000
2890540	-225154185656400	18316448212957609228	-52049186274422708166126 96	
-383820	45013264977235	-79941030264677325 72	42774185775282548246302 50	
21408	-5334575903403 12	25880040094463959 64	-27183271813155842882496 60	
-288	412890817060608	-61370395818658218 8	13477175108324548874804 84	
	-217302832717740	10374685205441318 4	-52218948513342605484198 4	
185794560	78674484241229	-11900436822031936	15734821491298487645376 0	
-501250680	-19411026117032	84612340491379 2	-36421204864054622088184	
573258726	3158693692628	-30888534752640	63359369952279225931 04	
-353443272	-316070322480	32606945280 0	-79927831885190140128 0	
124552532	16764887376	-40642560 0	68948045964588714048	
-24722336	-321615360		-36673405477538734 08	
2557496	1036800		964365197414630 40	
-110976			-5101837332480 00	
1152			263363788800	

Table III. *(Continued)*

--- KLAUDER MODEL ---

SECOND MOMENT ... DIMENSION = 2

2			7925512637817815040000	5102165312251656929280000	
			-39310816550009274270000	-31780842488777945482920000	
16	37158912000	19996607722291200	9126703886472549118350	938964038432810175756936000	
0	-829103688000	-748575276937488000	-13111357287504418462440	-17443395444011411423013191200	
	80536133880	12851645343191466660	12994226681864595109848	22785181141211991642331272160	
144	-43897168344	-1330397127994388804	-938371991064763223208O	-22179664585263629153769831136	
-24	14541877408	92027136509367096	5085937275352106554652	16641823296354679178260348800	
2	-2970973696	-445982216511969952	-20995197450094117104240	-98204896379147816369740652 8	
	360901984	154447647593991404	662505311760664611348	46087881344403304656216944O	
1536	-23195712	-38240146411957160	-15872984224434407834880	-17273365304729489589849356 8	
-576	562176	6644981016064000	283471351269602099760	5159371986341442132316134 4	
64	0	-776008624740160	-36468208155036896640	-12176258295244090360739776	
0		55952759575680	31878684585799635200	22339586582995494952862720	
	899245670400	-2087641981440	-17087863576002048000	-31035270353330890870720000	
19200	-2333922822000	24380006400	4581082507852800000	31331217174999103322112 0	
-12120	2684304031455 0		-3382622208000000	-21516045263505710899200	
2678	-1777661700342		32514048000000	895879039240605450240	
-224	741381823643	642748105359360000		-17732555598038630400	
8	-200588718352	-26625958486447320000	3021018934885849497600O	5969311668633600	
	34905187416	5098856393907541912.5	-16245887074746417690280000	0	
276480	-3705163000	-5948448512623975215	41097259452685948568000		
-252000	211870592	469733333419427831 5.5	-64721936946672621784764O	22500549027029807058124800O0	
85944	-4963200	-26411923610491687 98	-56957677880902519224115 2	-14989511641628050641264150000	
-12472	28800	10834265251823682O6.5	-16892694104979739206016	4752883026024123695865694537 5	
704		-32656007834808022 9	3666380009728156938656	1733314363920816399421179735 9	
0	23543886643200	71757069884339344.5	-59707737829827349856O	-76480800404946061305512745072	
	-69902679369600	-1120858429423374 4	7033149256086113331 2	40013496164024554141177461788	
4515840	93229805727360	1184201691014744	-56386077514049587 20	-16906231344657105462529821648	
-5498640	-72937258875360	-772314455220 48	2764337007995965 44	5772043638310586593944472032	
2665035	36806257776192	259860459556 8	-66260560442572 80	-15846844027426868122390724 24	
-628534	-12433798033888	-2868929280 0	34895934259200	3466654787838663458093097 48	
74409	2824614243264	5080320 0	0	-59024583994386572629930032	
-3840	-420666903360			7642735888722352887110672	
72	38403397376	21939135329599488000		-71927286468423008496789 6	
	-1849816320	-99778459277008512000	12117642616597685207040O0	45914393273846861463552	
82575360	31150080	21117550130034755040O	-70292673840874597732620O0	-17653995583423837774720	
-127169280	0	-27455620135671171648O	19266429221920D335126300 75	32043340388630937600	
80941632		24408721033236080812 8	-33051612061685551246119990	-9585141814886400O	
-26643712	663152807116800	-15642657789697112448O	39653378955075601008531081	26336378880000	
4743360	-2223174760606800	74254036807965653824	-35230579545746250131801976		
-430336	3386572235831835	-26406653309892943616	23950620881490696583310634		
15360	-307346018297868O	70271750555305077 12	-12695128010149654252158268		
0	1836017281036656	-13799686421493155 84	52959407101453430824171 16		
	-754076774526988	19408382163551795 2	-17416733309898863733848 64		
1672151040	215986419789445	-18525406972796928	44898496365218852518740 8		
-3143017080	-42760245203368	1088831742529536	-89468558569073685298936		
2517065190	5645807286996	-32228795842560	13447264939329779575632		
-1095991368	-460583550768	25639649280 0	-14651318371632651373 44		
278184788	19911764304		10848772264873380768O		
-41029280	-321615360		-48829484457414696 96		
3241016	1036800		10658896320211200 0		
-110976			-5101837332480 00		
1152			263363788800		

Table III. *(Continued)*

--- KLAUDER MODEL ---

1

SUSCEPTIBILITY ... DIMENSION = 3

4

32	3805072588800	2340174435157278720
-4	-5809024998000	-5524520276447172000
	4004859852900	6180402174707747217
384	-1583181474372	-427289308273568892
-96	381701048304	200508929742068819
4	-55846621208	-663101543242056349
	4708442912	156064574500554085
6144	-203183696	-259017196927620782
-2532	3429888	294922495125849
312	-17520	-2185671494442968
-8		95785204884768
	167423193907200	-2063007440928
122880	-289470905539200	14507458560
-70560	229525666263810	-14515200
14116	-106953501915876	
-928	31505106209410	1404104661094367232000
16	-5931076914752	-3615224983017455808000
	695296501944	444091084543528851712
2949120	-47639291216	-340449858822808703367
-2228400	1669217152	179511473004043357572
655500	-22218240	-678753642152995098108
-83668	57600	186831412923671189059
4064		-373688716429711365654
-48	8036313307545600	53440531037065676677
	-155731011512076000	-528693252379581824
82575360	14033187340375860	34127574178435984
-77374080	-7595424942343812	-1295573831659008
29791038	2682042914332932	23678281284768
-5546108	-632644560885028	-13163544576
477174	98803510440096	101606400
-16416	-9845745290304	
144	579926009120	898626983100395028480
	-17327707968	-2509851842717769454905
2642411520	188167680	336546579037374906921
-2987695620	-345600	-284208052839624736875
1451389704		167111768473816126095
-371235528	417888291992371200	-715963302047143859412
50714184	-8970831394997200	227911735914367036901
-3422408	904373593269334470	-541114217062859617479
93120	-5558415491908836	9501433970472082695
-576	2275551447340740	-120809536503512070
	-640146768552960	10709490914057604
95126814720	123941084567586	-62061910890114982
-12597914448	-1618395941100752	2100136154349542
73613891268	1362597472605	-333473468739840
-23716082928	-67893456991	1502590279680
4386813688	169370009568	-812851200
-450124768	-1460920320	
23353552	2073600	
-486912		
2304		

611066348508268619366400	267500404722979670813835264
-184005259348696969102920	-98425169381144624141680256
267299597063023426020357	17674009324357945324730083
-246225113959315633906748	-20451944104299656611175521
15935607760296361911775056	16982085409219384565695646
-760215034352366183966428	-10674440436302687422016229
27342286064829438016756	52283354828982778692477
-74714023068699130887288	-20261279827424838063992
15462758387132023096264	62517829359609517234248
-23921596517717508393376	-15352052180573627357418
26981815021172323422	29802633769807974055522
-21280488053159914176	-45128970728405259918867
10952407535705587072	52158089762461800214297
-32616867956128358	-44498052064707171826966
4440558911800320	26618457769008820919477
-15623278755840	-10279545395706335915136
6502809600	22163081002369933536
	-19772981297069045760
43996777092595340594380	34113854354227200
-14223980979017436503576	-5267275776000
22285644053336408276164	
-22283607787892430278008	22470033996730292348362
15788102466455717269935	-87726972807535156699264
-83348821619829376862050	16761141623247394292679
33625219921741382926327	-20714379902282679980085
-10480147365244141200031	18457938729285463112489
25259645912062121059750	-12525054436251086086965
-46727272557188253803071	66709790003530322460638
65249885367556130620400	-28358507657349172548329
-66861049724651632933904	97004693686763910323854
48040348562414111750016	-26748743551100902875551
-22475612683261003200	59243953785082719103256
60181999098444654	-10443983991408346853711
-7137731477445120	14429800595069040172392
201735919042560	-15259335657294365700744
-58525286400	11920720870920983333349
	-65189704233535489645576
33437550590372458851729408000	22893930964505849170314
-11551683296545805336124801600	-44324794445924996720640
19409751788771301072831207765	34294881336676024320
-20917712240340588830801853234	-44569630870732800
16076849788661245087265563159	52672757760000
-92820118165106922764308770336	
41365785461227061410709299284	
-14419227651763636547455830728	
39467808036252473903607036	
-84528920629753852449787478	
14012759679999353521774112	
-17634840213342700992834416	
16334048259889704823177	
-10608312413319131596070	
44680824185593525044	
-10650306480046157721	
10905501241653811	
-2366229165834240	
526727577600	

Table III. *(Continued)*

--- KLAUDER MODEL ---

SECOND MOMENT ... DIMENSION = 3

4				
64	38050725888000	32762442092201902080 0	1038812792464056652922880 00	5350008094459593416276705280 0 0
0	-419239364544 00	-60138415002990804480 0	-25148558726067289965051600 0	-16197941329068777691605768576 0 0
	20696365325520	51990932102115574260 0	2921634170459211020955813 00	2381214774040378249705081111144 00
1152	-5817225110736	-27653026759995293272 8	-21446161325801924723140536 0	-22473089526285353623622289863 0400
-96	997575636352	99722653604894451552	1105050323457068357194457 76	1519039101434247609704749678757 440
4	-104797988224	-25424047430625157904	-42069725785888318889890464	-77759274785196411145513912406976
	6427435456	4647022191141516872	12145267363134458319240856	3110509879437018869904142505472 0
24576	-200961408	-605213648263155800	-26877121348737515502225 12	-98950359128792717397533375674 88
-4608	2248704	54662345994772032	4555036960372176910314 48	2523804608412088813840118854720
256	0	-32388052788362688	-58391887024684851994528	-51644889868606723610504237882 88
0		1135493376764 16	5517377225152295697360	8424294444393239939588397030 4
	1841655132979200	-19210320276 48	-36773658742388809612 8	-10800804462706994243227707776
614400	-2355847403817600	9752002560	1609411343351688947 2	1063343768403093459316626432
-193440	1373765554847250	0	-410110621096790016	-77567599468781529491028480
21796	-469160663845764		486594911107584 0	3970260830527719271145472
-928	101744679146482	21061569916415508480000	-15623278755840	-13072172920608873443328 0
16	-14321407168640	-42712473333531089088000	6502809600	2377111289953871314944
	1288102999128	41098256993005091313525	791941987666716130698854400 0	-17447975700329594880
17694720	-69587195216	-24591193642057686930630	-20756638017389685129919200000	2387724667453440 00
-8029440	1976183680	10118612782781903824875	26223636831328011473147408400	0
1399536	-222182840	-29979713642809076251 80	-21061429762804331986891809360	47187071393133613931560540569600 00
-101968	57600	6522154540446845 6835	11965888269916883070820985376	-15259813562021002946529073916400 00
2816		-10439145395070147599 0	-50708310167000032355135959 04	24032958164564745903672243082142 50
0	96435759690547200	12119565142839883395	16484932570221543355480781 76	-24395978290655524257981580875013 800
	-140869882315008000	-98696976283511360 0	-41669134169871243875733320 32	17825168953889710204681186268623 200
578027520	9503905407328224 0	5305639294858216 0	821258504639968412098975 36	-99234512483047866269951501139 67800
-349614720	-38310944925407616	-16946262868514720	-12535346948310331430551168	43488002935883635078977491384 67354
86612670	10069073151586560	2652556477968 0	14565876999497050063300 4	-15290505267864252830166162069 02496
-10439164	-1777172743470784	-131635445760	-12503289344766400279155 2	43570952505452412129183155684 1808
631286	209905472202624	101606400	75540787060861709557 76	-10094079352601413699239051085 8912
-16416	-16012740779904		-29700493289148698479 2	18954273841296547606672131225 384
144	726959395328	14378031729606320455 68000	66312515018391920 64	-28579128191765952205557834916 32
	-16526298624	-31963470911722204505 6000	-64060836977295360	34034285907368327559191685602 4
21139292160	124600320	33920142532088468072 25600	139583737036800	-31208114385698684281135830432
-16139612160	0	-22577305780089540131040 00	0	21220046255371732262730489 28
5243010816		10448560994304074239952 64	6353134612170767181828587520 00	-10113541510963323888858777 6
-885776768	54325477959008256 00	-35299994179419926610355 2	-17937090002026811047282250400 00	30938552374934819927024 64
80251776	-894483640010600640 0	89078989658348243387392	24506755487974990740313135300 50	-52286609025959820503040
-3617280	68765793249735308 70	-16902340791295937763200	-21398739577539054750479678387 40	362254174594405171200
61440	-32115107082236661 36	23950544990136257544 96	13307188124369606690201224272 30	-44569630870732800 0
0	10002341122476355 44	-24810224100732201267 2	-62034172275956634946205323 84	52672757760000
	-21566717622443711 2	18051288337765571584	36379350408948140929561143 2	
856141332480	32454198934612350	-86136039724849766 4	-38941647547270643414825840	
-79614012240 0	-33551709087267 36	23901413131247616	30896565784971962715089 60	
3247477808 04	22788895577693 6	-30461673701376 0	-17266458147184927762828 8	
-72854864112	-93156781295 04	10255859712 00	62724457069132872418 56	
9536197432	19454502499 2	0	-12943438984039896576 0	
-721022944	-14609203 20		11717696718505728 00	
28821712	20736 00		-23662291658342 40	
-486912			52672757760 0	
2304				

Table IV

--- DOUBLE GAUSSIAN ---

SUSCEPTIBILITY ... DIMENSION = 3

1			2251799813685248		1152921504606846976
6			-7991546340523392		-5060293482378411328
0			5593532230176768		3831617245104001536
64	1073741824	4398046511104	68177920852996128		5531467324162891305 6
-8	-1850020288	-120550359843 84	-2009226079723724 80		-1779486596008010 69056
0	922789376	75853744168 96	-6742176455693583 36		-7846153612513529168 64
512	6552537248	75598550409312	5669472064548790272		7124053190207570909184
-128	-12979476480	-1974238122352 64	-4521887799784074240		-3696093006579317989120
0	-15185726080	-4653198145721 60	-9679630212914292326 4		-1961820814294461645 76768
32	83297243136	3496391318403072	4403685380344903434 24		984217456958806432733184
4096	-55325596672	-3218740746062848	-3088882598499083878 4		913006172166214281592832
-1752	-168711585792	-30982567552712704	-6036287503946395967488		-2988623922518112273068851 2
256	2706176611440	11562041856605798 4	2026874679510775391846 4		1204985051232484127090933 76
896	-73678716928	-6420136409989120 0	-7146753627112991293440		4268084590391258456293375 0
-256	8589934592	-4630323635372134 40	-1150166543410446876016 64		-2199369992773710513779900416
32768	-16892673024	1014329591640096768	3080463651224079215493 12		8495724965423963562305323008
-19840	9016074240	-4106788599409049 60	-3245554733551501317242 88		-1018525797015828677974933 2308
4096	70667322720	-4139339953474109 44	1537242715114421878784 00		-2182697517632752872787122585 6
17952	-152325988352	35184372088832	1801439850948198 4		8456698839190966592880613785 6
-12288	-219936971520	-1057385616865024	-6894442880076256 0		-7936748271369828932241902796 8
2048	1331230408704	691345489264 64	4972462827274393 6		-7662205947008005355333484544
262144	-978669761792	740691953012640	6426038374241288 00		92233720368547758 08
-213312	-4541593911296	-2021864203952128	-1957585138567510016		-43098974436857533440
62976	10334897553408	-5425292043341568	-7241633258043905664		3337176458517827584 0
282528	-6273850933248	42470818511208448	6278618750172480512 0		5064367769308517903 04
-281600	655326101504	-378506324865006 08	-4575181792358804244 0		-1666819492546440577024
-68992	68719476736	-4819098027626987 52	-1276113952490122969088		-7957252762264565522944
108544	-152670358976	19477514266191380 48	6067598022339080749056		7355942600601613264486 4
2097152	87071564288	-9059587391368069 12	1234828368015311437824		-2840967997878704938438656
-2143232	741573039008	-1233359737933219 0208	-1129350790051351923671 04		-2313505907075902834999296
745472	-17263932416 00	3177708408518213632 0	4159193738787245326336 00		1177563236083652478863769 6
3900000	-3002210792320	-9969306040818434048	-1213597452661871144623 36		1632052722978263361729331 2
-4997120	19991317775360	-6158213465731076992	-3498957391443372741492736		-4395306487086130595291910 4
-1858304	-17203499782400	7266854166471793049 6	1099715588876940120345804 8		1802068960049322345411903488
4673536	-96726017736704	2814749767106656	-1213289877827482657646182 4		1626479873018664492111757312
493312	27533626870 4608	-9224257137428 08	-6485312657115348824227 84		-4582840848392254051899198668 8
16777216	-156929310949376	6261339600919 04	6828753732491547057848320		1874667436946428150298540769 28
-20982744	-2403934612357 12	7161403050290304	1441151880758558572		-2103637675185662052129335279616
8595712	2248365514423 2	-2038970210834 5088	-5916518950187037 872		-9020416651132040243841450639 36
49345152	549755813888	-6143637169351 1808	4376079896325898 24		3653617068436474884063311691776
-76353280	-13615946700 80	5014472307957529 60	5985330875493408992		-3510281825667641918015362039808
-50704256	8161162772 48	-4356636818980958 72	-1874553490784616 4480		-5806840227814029089422991949824
193463808	7556781305312	-7049253228804993 024	-7599793782394089344 0		1301878076525732593876470018867 2
-65150720	-186676941373 44	3061888217419009 4336	6740676377104619724 80		
-67588096	-38150563463680	-8956333504502915 072	-4202877068284772134 40		
134217728	269837968338944	-3020314555107857 73568	-1605465363192280491622 4		
-198557056	-237723565958144	9326588332833951907 84	7842531506283702750412 8		
89821184	-1825020772679680	-4889464717797183815 68	4280273864708862672896 0		
581508128	6030723630456832	-2687794580495873802240	-1882183024291353754542080		
-1027452928	-3885809656070144	5266221037285522374656	7235439790407158537125888		
-913625600	-10602265088356352	-2646091981768197406720	3066015023986204249292 80		
4217683968	14863430695518208		-9447585904958137280443187 2		
-1743363584	2124252676096000		3360857991275844498902220 80		
-5354061824			-4432219086104203116853329 92		
5154897920			-7222377170463124402837913 6		
			4961161982999684295499448 32		
			2475258959328441884400199168		

Table IV. *(Continued)*

--- DOUBLE GAUSSIAN ---

SECOND MOMENT ... DIMENSION = 3

8			38280596832649216	2305843009213693952	0
0			-105317652543913344	-8039729876197645516	8
128	10737418240	61572651155456	564727402923663 36	480083002864252355 56	0
0	-12828918784	-126328035385344	708281407618502688	706245139319314331136	128
0	4219305984	58277248565248	-159409776673638400 0	-177865955049704774041 6	0
1536	33037705856	6079940568334 08	-621965161433462220 8	-881480065075043764224 0	32
-128	-44421873664	-1167385599344640	364856593656708710 40	583153569841912252170 24	16384
0	-72786672128	-3380981645765120	505257984184959482 4	277903743753741575249 92	-3072
32	219644084224	16486588550627328	-570113743111408287744	-144483261915888254494720	0
16384	-14720024576	-1009739379814400	157713862091765818982 4	449244005676456398458060 8	1024
-3072	-430966964224	-137302282608967680	269987957090621089382 4	151450010944744949190492 16	0
0	355488563200	29512199122211 6352	-249895858204018695225 6	-150061453315623696384000 00	32
1024	59016216576	189085772265553920	422643308844078016757 76	296111619516720137109504 00	16384
0	94489280512	-150616866987158732 8	762577313761755862794 24	129414985269128571392727 4496	-3072
163840	-132231674880	158176466917392384 0	-409196825466956382470 144	-870423968021871382958073 4464	0
-52608	48519077888	550189910840770560	596450144473479612923904	161275374284887761535940 68992	1024
4096	409286519904	-945827526981186 32	-331269325640611343106048	176032722049565551777745 46944	0
30240	-617813516288	527765581332480	189467607868861721870336	-125739038156102997391553 069056	163840
-12288	-1194424750848	-120350485883289 6	324259173170675712	183827255794294310903010557 952	-52608
2048	4258627977216	587583979192320	-970405961799681024	-348637243645261881236017 64352	4096
1572864	-388596264192	65372967506610 24	541278438021758976	-723503313631719950480530 47296	30240
-738304	-13869117571072	-133304901142528 00	717774481412723520 0	193690812773950291968	-12288
98304	18202695745536	-429709808229537 28	-168350413290324951 04	-72414308581386622259 2	2048
643200	-2983185088512	225257915098120192	-715411377200351191 616	445445078213065908224	1572864
-360448	-305251237888	-31368091498969 60	438954759631281782784	687826964947078854934 4	-738304
-167424	824633720832	-237505837005792870 4	105083123871903414272	-178659759455552440967 168	98304
163840	-1328136167424	569962576038260412 8	-811215202346986504192 0	-949492975878319514711 04	643200
14680064	532409810944	51752358431077826 56	235323014530060591104 00	648425243940779157159936	-360448
-9319424	4836896022016	-446239293894767861 76	521161532799946928947 20	396450065700985580687360	-167424
1794048	-8005282856960	5172615794672323788 8	-493946458508037772181 504	-182799073424664104953446 40	163840
11500128	-18051399663616	601843786849333493 88	905790754595069864443904	581821423871084250438947 2	14680064
-9191424	72889338462208	-200744696384485588992	216137197311448308099973 12	235306828386630542718926848	-9319424
-6109952	-7491825778688	155765643432962785280	-127404673479256967342981 12	-237289146662545288220581 4784	1794048
7294976	-338641229185024	4503599627370496	195246199670304822567895 04	471385281493996281911286 1696	11500128
2787072	531596922093568	-113198551405035 52	-339732751146831959966089 216	271800199930891790912061 4400	-9191424
134217728	107159846912000	5806824616361984	255111954724057586209914 88	-191612938433059688015638 036480	-6109952
-108847104	-74832089776128 0	6870180046679347 2	37609776349735234844951 4455040	376097763497352348449514 55040	7294976
26279936	40458112624230 4	-14756131457567948 8	663967821577607058438284 90240	663967821577607058438284 90240	2787072
178412544	7146825580544	-52560627475279257 6	-473341909486411274722960 4741120	-473341909486411274722960 4741120	134217728
-17501388 8	-13067815083008	2924813605577326592	745419383038470087964622 00091392	745419383038470087964622 00091392	-108847104
-182278144	5652423516160	165070429446483968	543918571856752004630365 3396480	543918571856752004630365 3396480	26279936
333987840	55099463643360	-37926042099932725248	-335168940910020308255327 96436480	-335168940910020308255327 96436480	178412544
-4657152	-98874934829056	981262530055070679 04	391846160057344333540004 38919168	391846160057344333540004 38919168	-17501388 8
-72482816	-2538541135549 44	128732575626208477 184			-182278144
1207959552	1138888819372032	-113878297504688426 1888			333987840
-1206500736	-107866133595136	173409257251702256 4352			-4657152
347770880	-72783584703938 56	200457058646006143 3856			-72482816
2522266656	1390591944244 4288	-893627024607339662 5408			1207959552
-2969939968	411043981433241 6	795683717161080428 9536			-1206500736
-3897152000	-356427581627064 32	316468966927324151 808			347770880
9566863360	183607814436945 92				2522266656
102822400	24001892001251328				-2969939968
-11615109120					-3897152000
7973470208					9566863360
					102822400
					-11615109120
					7973470208

Table V

SPIN-1/2 ISING MODEL X SERIES

N	C(N)
0	1.00000000000000000000D+00
1	8.00000000000000000000D+00
2	5.60000000000000000000D+01
3	3.89333333333333333333D+02
4	2.61066666666666666666D+03
5	1.74730666666666666666D+04
6	1.15250488888888888888D+05
7	7.59545701567301567301D+05
8	4.98669457777777777777D+06
9	3.24588052119929453282D+07
10	2.11100973265044091710D+08
11	1.37234112696909411576D+09
12	8.89225340465801720912D+09
13	5.75990465873023621645D+10
14	3.72215887749060899923D+11
15	2.40468209448518742434D+12
16	1.55077634970517388867D+13
17	9.99873514610603599664D+13
18	6.43783386253783878175D+14
19	4.14433354923102785140D+15
20	2.66494514146530495988D+16
21	1.71338208774669517510D+17

COEFFICIENTS GENERATED BY RECURRENCE

	XD/DX [9,6,9;ϕ] APPROXIMANT	D/DX [7,6,7;1] APPROXIMANT
22	1.10059191092457497919D+18	1.10059193060782825513D+18
23	7.06871245265672425026D+18	7.06871262207970993318D+18
24	4.53655580392347726330D+19	4.53655620300683080303D+19
25	2.91113087659445828831D+20	2.91113119320523868716D+20
26	1.86689475194048249434D+21	1.86689520552139038074D+21
27	1.19710894245379829435D+22	1.19710928632091991155D+22
28	7.67202488600133011304D+22	7.67202877778161457777D+22
29	4.91639971158562724207D+23	4.91640258370356403918D+23
30	3.14904413998220708426D+24	3.14904697047578655365D+24
31	2.01685853368627561650D+25	2.01686058578308720264D+25
32	1.29119573988069229256D+26	1.29119858745841407276D+26
33	8.26567133139960196551D+26	8.26568455103175985501D+26
34	5.28938857674719571543D+27	5.28939975099876789728D+27
35	3.38457862981850481481D+28	3.38458654106215848884D+28
36	2.16502613059527469107D+29	2.16503251632024768462D+29
37	1.38462865359771898696D+30	1.38463333470200275619D+30
38	8.85530288524326863560D+30	8.85533781493800204543D+30
39	5.66222914056120751295D+31	5.66225346593933761440D+31
40	3.61958283574239291860+32	3.61960128962965673779D+32
41	2.31370660202349556233D+33	2.31371936836090447424D+33
42	1.47861801123903165300D+34	1.47862748950904773207D+34
43	9.44896241828766730988D+34	9.44902760596841896142D+34
44	6.03697784210262994602D+35	6.03702540217781581126D+35
45	3.85688772036886379577D+36	3.85692026081452886790D+36
46	2.46359832195059892680D+37	2.46362172419743652578D+37
47	1.57357016668179882393D+38	1.57358610436800868989D+38
48	1.00490486520117478549D+39	1.00491619052061814164D+39
49	6.41724029075325745655D+39	6.41731709972998321726D+39
50	4.09732626692191953513D+40	4.09738029739437174825D+40

CRITICAL PARAMETERS

XD/DX [9,6,9;ϕ]

K_c = 0.15737356
γ = 1.23756
θ = 0.50000
α = 0.14665
A = 1.04028
σ = -.10640
B = 0.

D/DX [7,6,7;1]

K_c = 0.15737288
γ = 1.23720
θ = 0.50000
α = 0.10515
A = 1.04210
σ = -.11272
B = -.22324

RECURRENCE RELATION COEFFICIENTS XD/DX [9,6,9;ϕ] APPROXIMANT

	Q(0,J)	Q(1,J)	Q(2,J)	P(J)
0	0.	-4.16841603697922105464D-01	1.00000000000000000000D+00	0.
1	-4.86526717041662315629D+00	2.19920288156373658058D+01	-1.00816695313780467566D+01	0.
2	-2.35274477296574291331D+02	-1.11372248724797869848D+02	-3.63394020202092635717D+01	0.
3	1.03201726672452817176D+02	-1.74479540856078525368D+03	6.77459010723451448509D+02	0.
4	1.55402816608140504445D+04	8.40368131213591118195D+03	-9.34015050746944594742D+02	0.
5	6.05672264274075353273D+03	3.70316485357376837901D+04	-1.34566970120547120030D+04	0.
6	-2.16866153506778939883D+05	-1.45702331083651930366D+05	4.26172717831308881253D+04	0.
7	2.03571329121323151598D+04	0.	9.25266836211132046290+04	0.
8	3.77742836516401852439D+05	0.	-4.63824445533081678860D+05	0.
9	-1.92109048396973934321D+05	0.	4.02649840156050582146D+05	0.

RECURRENCE RELATION COEFFICIENTS D/DX [7,6,7;1] APPROXIMANT

	Q(0,J)	Q(1,J)	Q(2,J)	P(J)
0	0.	-1.00000000000000000000D+00	1.00000000000000000000D+00	0.
1	-5.64243806512001787986D-25	-8.10888355019796529687D+00	-3.87527167958427526710D+00	0.
2	-7.85464665102058630755D+01	-7.05923872002118138595D+01	-5.46328163855258213077D+01	-6.24197083484637875872D+01
3	1.29819847247994118537D+03	4.26841381750488465798D+02	1.65715223823586094664D+02	2.27769297863434263490+02
4	1.13878768881543349344D+03	4.43612601160676350090D+03	6.45235659575477682752D+02	0.
5	-5.83099082780388500007D+03	-4.74317700526347444363D+03	-1.57304626387865965127D+03	0.
6	-2.45990886464117050366D+04	-7.74851632876224648807D+03	-2.81207126214266173251D+03	0.
7	2.69916861892408178995D+04	9.00940946359766498725D+04	4.84494683139361767601D+04	0.
8	7.07661466262204161555D+03	0.	0.	0.
9	7.56714584509326345466D+04	0.	0.	0.